

Investigation of size-dependent quasistatic response of electrically actuated nonlinear viscoelastic microcantilevers and microbridges

Mohamed A. Attia

Received: 17 October 2015 / Accepted: 23 November 2016 / Published online: 30 November 2016
© Springer Science+Business Media Dordrecht 2016

Abstract This study investigates the size-dependent quasistatic response of a nonlinear viscoelastic microelectromechanical system (MEMS) under an electric actuation. To have this problem in view, the deformable electrode of the MEMS is modelled using cantilever and doubly-clamped viscoelastic microbeams. The modified couple stress theory in conjunction with Bernoulli–Euler beam theory are used for mathematical modeling of the size-dependent instability of microsystems in the framework of linear viscoelastic theory. Simultaneous effect of electrostatic actuation including fringing field, residual stress, mid-plane stretching and Casimir and van der Waals intermolecular forces are considered in the theoretical model. A single element of the standard linear solid element is used to simulate the viscoelastic behavior. Based on the extended Hamilton’s variational principle, the nonlinear governing integro-differential equation and boundary conditions are derived. Thereafter, a new generalized differential-integral quadrature solution for the nonlinear quasistatic response of electrically actuated viscoelastic micro/nanobeams under two different boundary conditions; doubly-clamped microbridge and clamped-free microcantilever. The developed model is verified and a good agreement is obtained. Finally, a comprehensive study is conducted

to investigate the effects of various parameters such as material relaxation time, durable modulus, material length scale parameter, Casimir force, van der Waals force, initial gap and beam length on the pull-in response of viscoelastic microbridges and microcantilevers in the framework of viscoelasticity.

Keywords Pull-in instability · Viscoelasticity · Microbridge · Microcantilever · Intermolecular forces · Size effect · Modified couple stress theory

1 Introduction

With rapid developments in nanotechnology, nano structures have been the interest of many researchers over the past decade due to their several enhanced properties. Micro/Nanoelectromechanical Systems (M/NEMS) have become one of the most important components in constructing develop micro/nano-devices like actuators, switches, biosensors, nanowires, accelerometer, tweezers, ultra-thin films, etc. This is due to their low manufacturing cost, batch production, light weight, small size, durability, low energy consumption, potentials as sensitive and high frequency devices, and compatibility with integrated circuits [1–7].

Viscoelastic micro/nano systems exhibit both solid and liquid time-dependent behaviors together to some extent. Viscoelastic materials can present interesting

M. A. Attia (✉)
Mechanical Design and Production Engineering
Department, Zagazig University, Zagazig 44511, Egypt
e-mail: omarmadly@yahoo.com

properties such as high damping characteristics, low weight, high strength and excellent possibilities to absorb energy [8]. Such materials are widely used in some technologies, such as robots, artificial biological parts, aerospace, automotive and dampers [9]. Experimental observations showed that when the internal material length scale parameter is in the order of structural characteristic size such as thickness of beams, the size effect is urgent and vital in their static and dynamic behaviors of metals and polymers [10–13].

A typical beam-type M/NEMS are constructed from two conductive electrodes where one is movable and the other is fixed. When direct current voltage is applied across the two electrodes, the electrostatic force is generated and the movable electrode is actuated to deflect towards the substrate. The critical voltage and the corresponding maximum deflection which leads the beam to be unstable and pull-in onto the ground electrode, are known as the pull-in voltage and pull-in deflection, respectively [14]. Therefore, predicting the stable actuating range and the pull-in instability parameters are important issues for designing stable and safe M/NEMS. For example, pull-in instability should be avoided in micro/nano mechanical resonators and micro-mirrors in order to achieve stable operations and enhance device sensitivity [1, 15]. On the other hand, estimation of pull-in voltage is essential to control the switch on and off [16].

It is worth noting that as the dimensions of electromechanical systems reduce, NEMS present monograph characteristics, which differ greatly from their predecessor MEMS as the dispersion forces (Casimir and van der Waals attractions) appear in a significant contribution to the NEMS behavior [17, 18]. At micro-separations (typically larger than a few nanometers while smaller than a few micrometers), the attraction between two surfaces could be described by the Casimir interaction [19]. It represents attractive force between two flat parallel plates of solids that arises from quantum fluctuations in the ground state of the electromagnetic field. On the other hand, the van der Waals (vdW) force can significantly influence the NEMS performance if the initial gap between the two conductive electrodes is typically below several ten nanometers [19].

Several models are proposed in the literature to investigate the pull-in instability of electrically

actuated M/NEMS devices. In this regard, the different nonclassical continuum theories are employed to investigate the mechanical performance of micro/nanostructures, in which material properties are highly affected by the dimensions and are size-dependent. These theories include some additional material constants besides two classical Lamé's constant for isotropic elastic material; the Eringen non-local elasticity theory which includes one additional material constant [20, 21], the classical strain gradient, the strain gradient, the classical couple stress and the modified couple stress theories of elasticity include five, three, two and one additional material constants, respectively [22–25].

Recently, the modified couple stress theory (MCST) developed by Yang et al. [24] has been successfully used to investigate mechanical behavior of microactuated beams as it overcomes the difficulties encountered in determining higher-order material constants by introducing only one additional material length scale parameter. Rahaeifard et al. [26] employed the MCST to study the size effect on the deflection and static pull-in voltage of silicon micro-cantilevers. Yin et al. [27] explored analytically the size effect of electrostatically actuated microbeams by using the MCST. Kong [28] presented approximate analytical solutions to the pull-in voltage and pull-in displacement of the electrostatically actuated microbeam based on the MCST using the Rayleigh–Ritz method. Baghani et al. [29] and Rokni et al. [30] analytically studied the response of electrostatically actuated microbeams and studied the effect of the applied voltage on the nonlinear size-dependent response of the microbeams. Static and dynamic pull-in instabilities of the functionally graded (FG) micro-beams subjected to a nonlinear electrostatic pressure and external heat source based on the MCST were studied by Zamanzadeh et al. [31]. Shaat and Mahmoud [32] investigated numerically and analytically the electrostatic behavior of microactuated cantilever beam including surface elasticity in the context of the MCST. Recently, this model was extended by Shaat and Abdelkefi [33] to study the effects of the material structure inhomogeneity of an electrostatically-actuated micro/nano Nc-Si cantilever beam on its pull-in instability and sensitivity to bio-cells are investigated. Wang et al. [34] analyzed the effects of surface energy and material length scale parameter on the pull-in instability and free vibration of

electrostatically actuated nanoplates considering the effect of Casimir force. Liang et al. [35] presented a nonlinear size-dependent model for the electrostatically actuated nanobeams incorporating Casimir force based on the strain gradient elasticity theory and Hamilton principle. The governing equations were solved numerically using the generalized differential quadrature (GDQ) method. Beni et al. [36] employed the modified strain gradient theory to study the size dependent pull-in instability of nano-bridges and nano-cantilevers, considering the effect of van der Waals intermolecular force. The Hamilton’s principle in conjunction with Euler–Bernoulli beam theory was applied for deriving the governing equation. Noghrehabadi and Eslami [37] investigated the size-dependent static behavior of clamped–clamped actuators in liquid electrolytes based on the MCST, where the effects of van der Waals force, midplane stretching and residual forces are included. The minimum total potential energy principle was used to derive the governing equation.

However, little attention has been paid for modeling the pull-in instability of the viscoelastic micro/nano devices with size effects. Bethe et al. [38] showed that for a thin silicon MEMS structure, the creep phenomenon of silicon became rather significant and consequently investigation of the viscoelastic effects in microbeams became necessary. The pull-in phenomenon of electrically actuated viscoelastic clamped–clamped microbeam based on the MCST was studied by Fu et al. [39], Fu and Zhang [40] and Zhang and Fu [41]. In these papers, the obtained governing equation was solved using Galerkin method and although the prescribed function in the space variable was chosen to satisfy the boundary conditions, it is not guaranteed to satisfy the governing equation. On the other hand, this approach is complicated if other sources of nonlinearity are added to the governing equation. Chen et al. [42] studied the buckling and dynamic stability of a simply supported piezoelectric viscoelastic nanobeam subjected to van der Waals forces based on the classical viscoelasticity theory.

This research study is the first attempt to analyze the nonlinear size-dependent pull-in instability of electromechanical viscoelastic micro/nanobeams including the simultaneous effects of material length scale parameter, intermolecular Casimir and vdW forces, electric forcing including fringing field,

residual stress and mid-plane stretching geometric nonlinearity. To the author’s best knowledge, no previous studies which cover all these issues are available. The modified couple stress theory is employed to express the microstructure effect of viscoelastic microbeams in the context of linear viscoelastic theory. The nonlinear governing integro-differential equations and associated boundary conditions are formulated using the extended Hamilton principle and Bernoulli–Euler beam theory in conjunction with the standard solid model of viscoelasticity. Afterwards, a modified generalized differential-integral quadrature (GDIQ) method is developed to solve the obtained governing nonlinear equations. The developed model is verified for both elastic and viscoelastic benchmarks of microbeams. In the framework of viscoelastic theory, a detailed parametric study is performed to get an insight into the effects of intermolecular Casimir and vdW forces, relaxation time, durable modulus, material length scale parameter, initial gap and beam length on the size dependent pull-in response (instantaneous and durable pull-in voltages, pull-in time, pull-in deflection and creep deflection) of electrically actuated viscoelastic micro-bridges and microcantilevers.

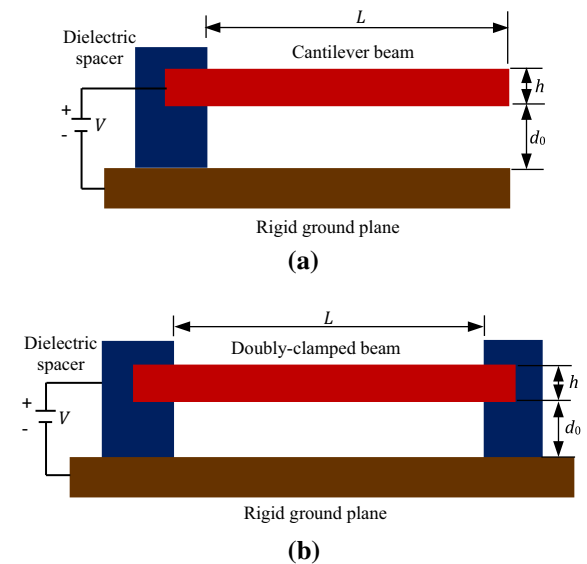


Fig. 1 Schematic representation of electrically actuated. **a** micro-cantilever and **b** micro-bridge

2 Problem formulation

This section is intended to derive the equations of motion and associated boundary conditions of an electrically actuated viscoelastic microbeams given in Fig. 1. The beam is actuated by a distributed electrical, fringing field, Casimir and vdW forces between a flexible and a rigid stationary electrodes. The actuator is modeled by a long and thin beam with the length L , width b , uniform thickness h , and an initial gap d_0 between the beam and substrate. The x coordinate is taken along the length, z coordinate is taken along the thickness, and the y coordinate is taken along the width of the beam.

2.1 Modified couple stress theory in the framework of viscoelasticity

The modified couple stress theory (MCST) proposed by Yang et al. [24] for an elastic behavior will be extended to the case of viscoelastic behavior of microbeams in the framework of linear viscoelastic theory. The nonclassical viscoelastic constitutive equations can be obtained based on the classical Leaderman viscoelastic linear constitutive equations, Phan-Thien [43], and the modified couple stress theory, Yang et al. [24], as follows:

$$\sigma_{ij}(x, t) = \lambda(t) * \varepsilon_{mm}(x, t)\delta_{ij} + 2\mu(t) * \varepsilon_{ij}(x, t) \tag{1}$$

$$m_{ij}(x, t) = 2l^2\mu(t) * \chi_{ij}(x, t) \tag{2}$$

where $\sigma_{ij}(x, t)$, $\varepsilon_{ij}(x, t)$, $m_{ij}(x, t)$ and $\chi_{ij}(x, t)$ are the Cauchy force-stress tensor, the infinitesimal strain tensor, the deviatoric part of the couple-stress tensor and the symmetric curvature tensor, respectively, and δ_{ij} is the Kronecker delta. The material length scale parameter l measures the effect of the couple-stress on viscoelastic behavior, Mindlin [22]. For simplicity, the length scale parameter is assumed to be time-independent. $\lambda(t)$ and $\mu(t)$ are the time-dependent Lamé’s constants in classical viscoelastic theory. Note that throughout the paper, the summation convention and standard index notation are used, with the Latin indices from 1 to 3.

The components of the infinitesimal strain tensor and the symmetric curvature tensor are defined as follows, Yang et al. [24]:

$$\varepsilon_{ij}(x, t) = \frac{1}{2} [(\nabla\mathbf{u}(x, t)) + (\nabla\mathbf{u}(x, t))^T] \tag{3}$$

$$\chi_{ij}(x, t) = \frac{1}{2} [(\nabla\theta(x, t)) + (\nabla\theta(x, t))^T] \tag{4}$$

where $\mathbf{u}(x, t)$ and $\theta(x, t)$ are the displacement and rotation vectors, respectively;

$$\theta_i(x, t) = \frac{1}{2} [\nabla \times \mathbf{u}(x, t)] \tag{5}$$

The time-dependent viscoelastic Lamé’s constants are given by, Phan-Thien [43]

$$\lambda(t) = \frac{\nu E(t)}{(1 + \nu)(1 - 2\nu)} \quad \text{and} \quad \mu(t) = \frac{E(t)}{2(1 + \nu)} \tag{6}$$

where $E(t)$ is the relaxation function and ν is the Poisson’s ratio, which assumed to be time-independent.

The Stieltjes’s convolution operation symbol ‘*’ appears in Eqs. (1) and (2) is defined as,

$$\mathbb{C}(t) * \mathbb{N}(t) = \mathbb{C}_0\mathbb{N}(t) + \int_0^t \frac{d\mathbb{C}(t - \xi)}{d(t - \xi)} \mathbb{N}(\xi) d\xi, \quad \mathbb{C}_0 \equiv \mathbb{C}(t = 0) \tag{7}$$

Consequently, Eqs. (1) and (2) can be, respectively, rewritten as

$$\begin{aligned} \sigma_{ij}(x, t) &\equiv \sigma_{ij}^e(x, t) + \sigma_{ij}^v(x, t) \\ &= [\lambda_0 \varepsilon_{kk}(x, t)\delta_{ij} + 2\mu_0 \varepsilon_{ij}(x, t)] \\ &\quad + \left[\int_0^t \dot{\lambda}(t - \xi) \varepsilon_{kk}(x, \xi) \delta_{ij} d\xi \right. \\ &\quad \left. + 2 \int_0^t \dot{\mu}(t - \xi) \varepsilon_{ij}(x, \xi) d\xi \right] \end{aligned} \tag{8}$$

$$\begin{aligned} m_{ij}(x, t) &\equiv m_{ij}^e(x, t) + m_{ij}^v(x, t) \\ &= 2l^2\mu_0 \chi_{ij}(x, t) + 2l^2 \int_0^t \dot{\mu}(t - \xi) \chi_{ij}(x, \xi) d\xi \end{aligned} \tag{9}$$

where λ_0 and μ_0 are the initial Lamé’s constants; i.e. at $t = 0$. The superscripts ‘ e ’ and ‘ v ’ refer to the current instantaneous elastic and history due to viscoelastic behavior, respectively.

2.2 Kinematic and kinetic relations

Based on the Bernoulli–Euler beam hypothesis, the displacements (u, v, w) of an arbitrary point with coordinates (x, y, z) are given by,

$$\begin{Bmatrix} u(x, z, t) \\ v(x, z, t) \\ w(x, z, t) \end{Bmatrix} = \begin{Bmatrix} z\phi(x, t) \\ 0 \\ w(x, t) \end{Bmatrix}, \quad \phi(x, t) = -w'(x, t) \tag{10}$$

where $(\blacksquare)'$ denotes a derivative with respect to the spatial coordinate x , $\phi(x, t)$ is the rotation angle of the centroidal axis of the beam and $w(x, t)$ is the uniform lateral deflection.

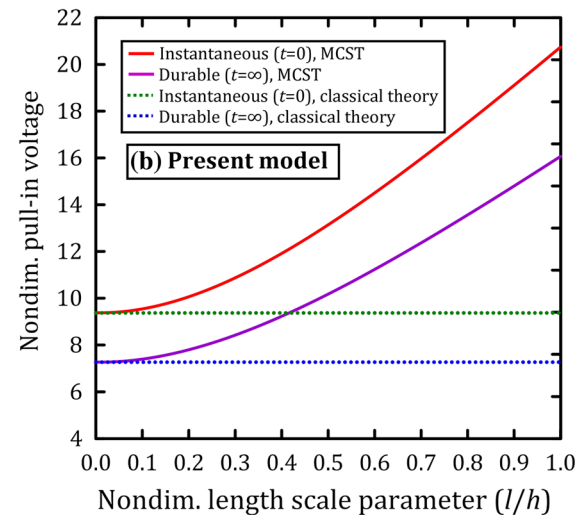
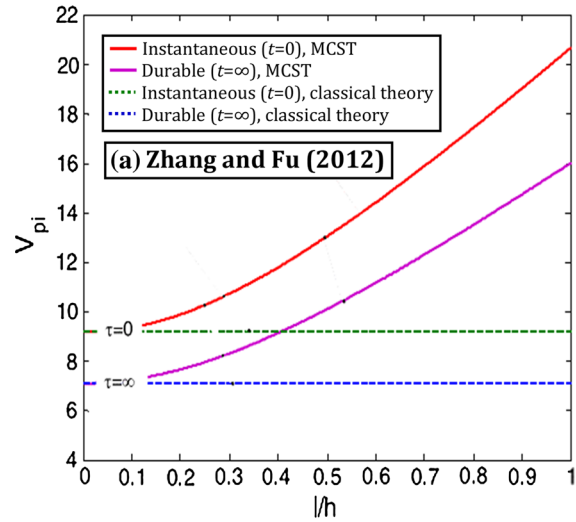


Fig. 2 Nondimensional instantaneous and durable pull-in voltages of viscoelastic microbridge when $C_F = C_R = C_C = C_{vdw} = 0$

From Eqs. (7)–(10), the following non-zero components of strain tensor, rotation vector and symmetric curvature tensor are, respectively, given by

$$\varepsilon_{xx}(x, t) = -zw''(x, t) \tag{11}$$

$$\theta_{,y}(x, t) = -w'(x, t) \tag{12}$$

$$\chi_{xy}(x, t) = \chi_{yx}(x, t) = -\frac{1}{2}w''(x, t) \tag{13}$$

Substituting Eqs. (11) into (8) and Eqs. (13) into (9), the following nonzero components of classical force-stress and deviatoric part of the couple-stress tensors are obtained as

$$\begin{Bmatrix} \sigma_{xx}^e(x, t) \\ \sigma_{yy}^e(x, t) \\ \sigma_{zz}^e(x, t) \end{Bmatrix} = - \begin{Bmatrix} \Gamma \\ \Gamma\nu/(1-\nu) \\ \Gamma\nu/(1-\nu) \end{Bmatrix} E_0 z w''(x, t) \tag{14a}$$

$$\begin{Bmatrix} \sigma_{xx}^v(x, t) \\ \sigma_{yy}^v(x, t) \\ \sigma_{zz}^v(x, t) \end{Bmatrix} = - \begin{Bmatrix} \Gamma \\ \Gamma\nu/(1-\nu) \\ \Gamma\nu/(1-\nu) \end{Bmatrix} \times \int_0^t z \dot{E}(t-s) w''(x, \xi) d\xi \tag{14b}$$

and

$$m_{xy}^e(x, t) = l^2 \mu_0 w''(x, t) \tag{15a}$$

$$m_{xy}^v(x, t) = \int_0^t l^2 \dot{\mu}(t-s) w''(x, \xi) d\xi \tag{15b}$$

For wide beam ($b \geq 5h$), the effective Young’s modulus can be approximated by the plate modulus, Osterberg and Senturia [44], such that

$$\Gamma = \frac{1}{(1-\nu^2)} \text{ for } b \geq 5h, \text{ otherwise } \Gamma = 1 \tag{16}$$

In the present study, the viscoelastic behavior is simulated using a single element of the standard linear solid model (generalized Maxwell viscoelastic model), in which the viscoelastic relaxation modulus $E(t)$ is given by, Schapery [45]

$$\begin{aligned} E(t) &= E_1 + E_2 e^{-\psi t} \text{ and} \\ E_0 &\equiv E(t=0) = E_1 + E_2 \end{aligned} \tag{17}$$

Table 1 Convergence of the linear and nonlinear pull-in voltages (V) of an electrostatically actuated doubly-clamped elastic microbeam when $C_C = C_{v,av} = 0$, $E = 151$ GPa, $\nu = 0.3$, $L = 5 \mu\text{m}$, $h = 1.5 \mu\text{m}$, $d_0 = 1.18 \mu\text{m}$, $\sigma_0 = 6/(1 - \nu)$ MPa and $l = 0$

L (μm)	Present model								Analytical, Rokni et al. [30]	Exp., Tilmans-Legtenberg [1]		
	N = 11		N = 17		N = 21		N = 31					
	Linear	Nonlinear	Linear	Nonlinear	Linear	Nonlinear	Linear	Nonlinear				
210	27.597	28.494	27.395	28.222	27.399	28.230	27.399	28.230	27.461	28.290	28.24	27.95
310	13.874	14.239	13.782	14.121	13.784	14.125	13.784	14.125	13.818	14.158	14.14	13.78
410	8.791	8.974	8.739	8.910	8.740	8.912	8.740	8.912	8.762	8.933	8.940	9.13
510	6.315	6.418	6.280	6.377	6.281	6.379	6.281	6.379	6.297	6.394	6.415	6.57

where ψ is the reciprocal of the relaxation time, E_1 and E_2 are the durable and creep moduli of the material, respectively and E_0 refers to the instantaneous elastic Young’s modulus.

2.3 Variational formulation

For a viscoelastic continuum, the extended Hamilton principle is expressed as, Chen et al. [46]

$$\int_{t_i}^{t_f} [\delta K - \delta \Pi^e + (\delta W_R + \delta W_S + \delta W_E) + \delta W^v] dt = 0 \tag{18}$$

where δK and $\delta \Pi^e$ are the variations of the kinetic energy and the total elastic strain energy due to bending incorporating the elastic part of microstructure effect, respectively. δW_R , δW_S , δW_E and δW^v are the virtual works due to residual stress, nonlinear mid-plane stretching, external stimuli forces and viscous dissipative forces including the dissipative part of microstructure effect, respectively. For the viscoelastic microbeam under consideration, these variations can be expressed as follows:

$$\delta K = \delta \frac{1}{2} \int_0^L \int_A \rho \dot{w}^2(x, t) dA dx = \int_0^L (\rho S \dot{w}(x, t)) \delta w dx \tag{19}$$

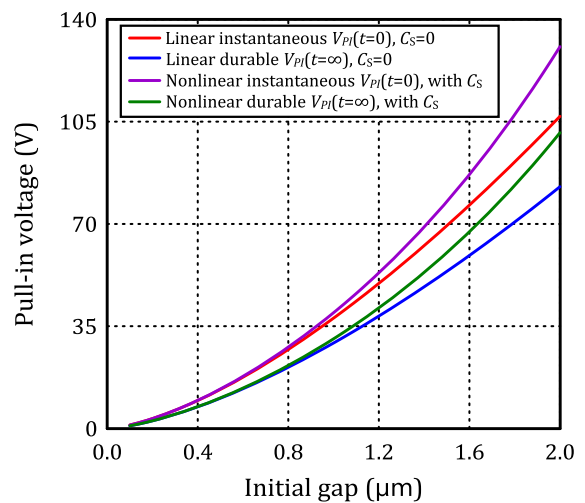
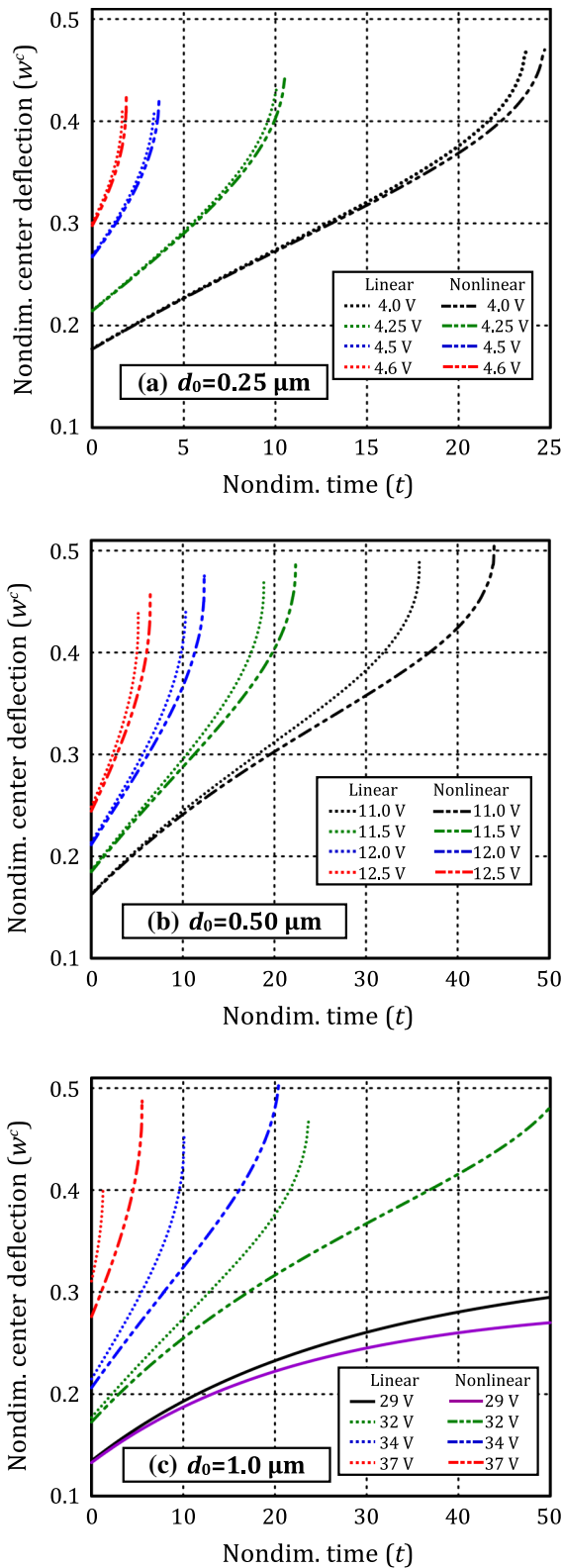


Fig. 3 Linear and nonlinear instantaneous and durable pull-in voltages of viscoelastic microbridge at different initial gaps



◀ **Fig. 4** Creep of the nondimensional center deflection of viscoelastic microbridge with and without mid-plane stretching at different initial gaps

$$\begin{aligned} \delta \Pi^e &= \delta \frac{1}{2} \int_0^L \int_A \left(\sigma_{xx}^e \varepsilon_{xx} + 2m_{xy}^e \chi_{xy} \right) dA dx \\ &= \frac{1}{2} (\Gamma I E_0 + S l^2 \mu_0) \delta \int_0^L w'^2(x, t) dx \end{aligned} \tag{20}$$

where ρ is the mass density, $S = bh$ and $I = bh^3/12$ are the cross-sectional area and the corresponding moment of inertia for the cross-section, respectively and L is the total length of the beam.

The virtual work due to residual stresses can be expressed as

$$\delta W_R = -\frac{1}{2} \sigma_r S \delta \int_0^L w'^2(x, t) dx \tag{21}$$

where the effective residual stress is given by $\sigma_r = (1 - \nu)\sigma_0$, otherwise $\sigma_r = \sigma_0$ for narrow beams ($b < 5h$), where σ_0 is the initial biaxial residual stress in the beam, Osterberg and Senturia [44]. In this study, it is assumed that the cantilever microbeams are free from residual stresses and hence δW_R equals zero.

The virtual work attributed to the nonlinear stretching force in the case of an elastic microbeam with immovable ends can be written as, Nayfeh and Emam [47],

$$\delta W_S^e = -\frac{1}{8} \frac{\Gamma S E_0}{L} \delta \left[\int_0^L w'^2(x, t) dx \right]^2 \tag{22}$$

Exploiting Eqs. (7), (22) can be extended for a viscoelastic microbeam as follows:

$$\begin{aligned} \delta W_S &= -\frac{\Gamma S}{2L} \left(E_0 \delta \int_0^L w'^2(x, t) dx \right. \\ &\quad \left. + \delta \int_0^t \int_0^L \dot{E}(t - \xi) w'^2(x, \xi) dx d\xi \right) \end{aligned} \tag{23}$$

Note that the axial resultant force associated with the mid-plane stretching is not considered in the cantilever case and therefore the virtual work δW_S equals zero, this is due to that the cantilever beam possess a movable end.

Considering the distribution of external stimuli forces per unit length of the microbeam (f_{ext}), the virtual work by these external forces can be expressed as

Table 2 Linear and nonlinear nondimensional pull-in time and nondimensional pull-in center deflection of viscoelastic microbridge

Applied voltage (V)	$d_0 = 0.25 \mu\text{m}$			$d_0 = 0.5 \mu\text{m}$			$d_0 = 1.0 \mu\text{m}$		
	No mid-plane stretching	With mid-plane stretching	No mid-plane stretching	With mid-plane stretching	No mid-plane stretching	With mid-plane stretching	No mid-plane stretching	With mid-plane stretching	
	$t_{PI}(t_{ss})$	$w_{PI}^c(w_{ss}^c)$	$t_{PI}(t_{ss})$	$w_{PI}^c(w_{ss}^c)$	$t_{PI}(t_{ss})$	$w_{PI}^c(w_{ss}^c)$	$t_{PI}(t_{ss})$	$w_{PI}^c(w_{ss}^c)$	
3.60	(186.5)	(0.321)	(182.4)	(0.317)	35.82	0.492	43.99	0.506	
4.00	23.70	0.469	24.70	0.470	18.84	0.472	22.32	0.485	
4.25	10.10	0.435	10.50	0.441	10.32	0.443	12.35	0.475	
4.50	3.40	0.412	3.65	0.421	5.14	0.436	6.44	0.457	
4.60	1.64	0.414	1.86	0.429	1.70	0.415	2.59	0.427	
Applied voltage (V)									
29.0	(195.4)	(0.339)	29.0	(148.3)	(0.290)				
32.0	23.700	0.469	32.0	53.10	0.565				
34.0	10.100	0.454	34.0	20.40	0.504				
37.0	1.250	0.402	37.0	5.52	0.486				

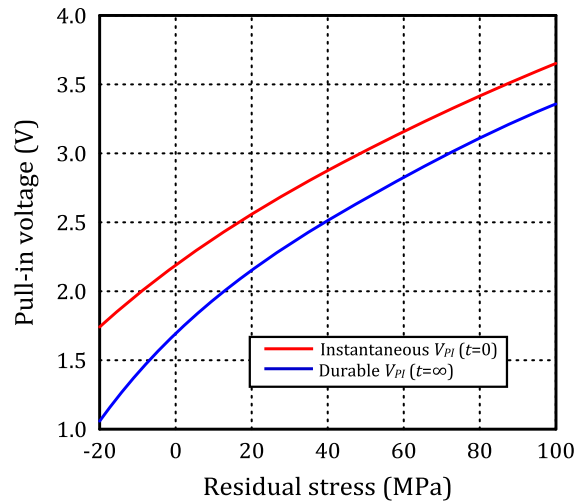


Fig. 5 Instantaneous and durable pull-in voltages of viscoelastic microbridge for various residual stresses when $C_{vdW} = C_C = C_S = 0$

$$\delta W_E = \int_0^L f_{ext} \delta w(x, t) dx \equiv \int_0^L [H_{elec}(x, t) + H_C(x, t) + H_{vdW}(x, t)] \delta w(x, t) dx \tag{24}$$

where f_{ext} is the consists of the electrostatic Coulomb force unit length of the beam including the first order fringing field effect H_{elec} and the intermolecular Casimir and van der Waals (vdW) forces per unit length of the beam, H_C and H_{vdW} , respectively. These forces can be written as the following, Huang et al. [48] and Gusso and Delben [49]:

$$H_{elec}(x, t) = \frac{\epsilon_0 b V^2}{2[d_0 - w(x, t)]^2} \left(1 + 0.65 \frac{d_0 - w(x, t)}{b} \right) \tag{25}$$

$$H_C(x, t) = \frac{\pi^2 \hbar c b}{240 [d_0 - w(x, t)]^4} \tag{26}$$

$$H_{vdW}(x, t) = \frac{A b}{6\pi [d_0 - w(x, t)]^3} \tag{27}$$

where V is the applied voltage, d_0 is the initial is the initial gap between the movable part and the fixed ground plane, $\epsilon_0 = 8.854 \times 10^{-12} \text{C}^2 \text{N}^{-1} \text{m}^{-2}$ is the permittivity of vacuum, $\hbar = 1.0546 \times 10^{-34} \text{Js}$ is the reduced Planck's constant divided by 2π , $c = 2.998 \times 10^8 \text{m s}^{-1}$ is the speed of light and A is the Hamaker constant with values in the range $[0.4, 4] \times 10^{-19} \text{J}$,

Batra et al. [50]. In the present analysis, all other external forces are assumed to be zero.

The virtual work due to the viscous dissipative forces including the dissipative part of couple-stress can be obtained as, Attia and Mahmoud [51]

$$\begin{aligned} \delta W^v &= -\delta \frac{1}{2} \int_0^L \int \int_A (\sigma_{xx}^v \varepsilon_{xx} + 2m_{xy}^v \chi_{xy}) dA dx \\ &= \int_0^L \int_0^t -[\Gamma I \dot{E}(t - \xi) + S I^2 \dot{\mu}(t - \xi)] w'' \\ &\quad (x, \xi) \delta w''(x, \xi) d\xi dx \end{aligned} \tag{28}$$

Now, by substituting Eqs. (19)–(21), (23), (24) and (28) into the extended Hamilton’s principle (Eq. (18)),

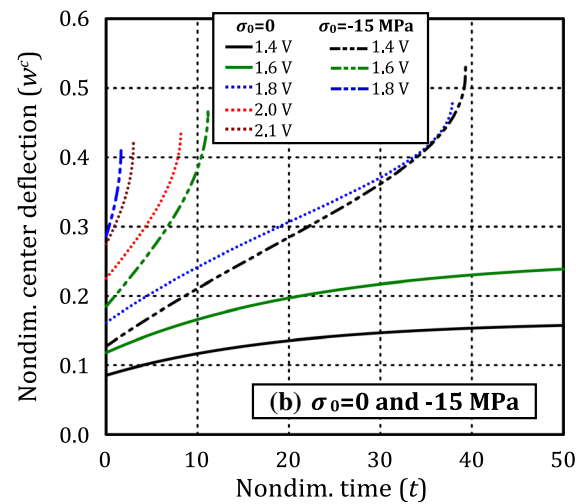
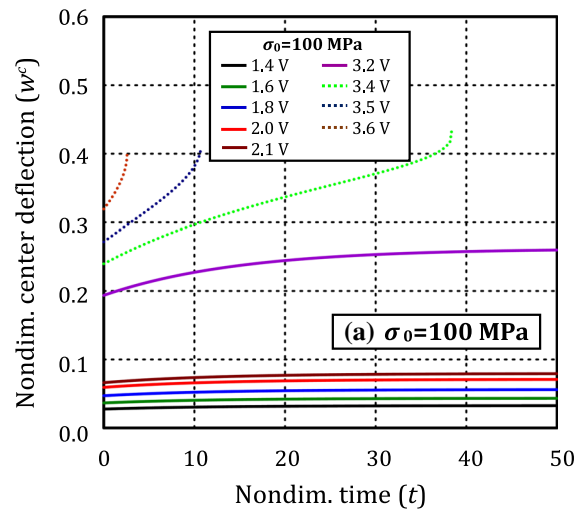


Fig. 6 Creep of the nondimensional center deflection of viscoelastic microbridge at different residual stresses when $C_{vdw} = C_C = C_S = 0$

while invoking the condition of zero variation at times $t = t_0$ and $t = t_f$, the integro-differential equation of an electrically actuated viscoelastic microbeam based on the MCST in the framework of viscoelasticity can be derived as the following:

$$\begin{aligned} \rho S \ddot{w}(t) + E_0 w''''(t) + \int_0^t \dot{E}(t - \xi) w''''(\xi) d\xi \\ - \left[\sigma_r S + \frac{S \Gamma}{2L} E_0 \int_0^L w''(t) dx \right. \\ \left. + \frac{S \Gamma}{2L} \int_0^t \int_0^L \dot{E}(t - \xi) w''(\xi) dx d\xi \right] w''(t) - \mathbb{H}(t) \\ = 0 \quad \forall x \in [0, L] \text{ and } t \in [t_i, t_f] \end{aligned} \tag{29}$$

in which

$$E_0 = I \Gamma E_0 + S I^2 \mu_0, \quad \mathbb{E}(t) = I \Gamma E(t) + S I^2 \mu(t) \tag{30a, b}$$

$$\begin{aligned} \mathbb{H}(t) &= \frac{\varepsilon_0 b V^2}{2[d_0 - w(t)]^2} \left(1 + 0.65 \frac{d_0 - w(t)}{b} \right) \\ &\quad + \frac{A b}{6\pi[d_0 - w(t)]^3} + \frac{\pi^2 \hbar c b}{240[d_0 - w(t)]^4} \end{aligned} \tag{30c}$$

under the following boundary conditions:

$$\begin{aligned} \text{Either } w = \tilde{w} \text{ or } E_0 w''''(t) + \int_0^t \dot{E}(t - \xi) w''''(\xi) d\xi \\ - \left[\sigma_r S + \frac{S \Gamma}{2L} E_0 \int_0^L w''(t) dx \right. \\ \left. + \frac{S \Gamma}{2L} \int_0^t \int_0^L \dot{E}(t - \xi) w''(\xi) dx d\xi \right] w''(t) = 0 \\ \text{at } x = 0, L \end{aligned} \tag{31a}$$

$$\begin{aligned} \text{Either} \\ w' = \tilde{w}' \text{ or } E_0 w''(t) \\ + \int_0^t \dot{E}(t - \xi) w''(\xi) d\xi = 0 \text{ at } x = 0, L \end{aligned} \tag{31b}$$

To transform the governing equation and associated boundary conditions into the nondimensional form,

Table 3 Effect of the residual stress on the nondimensional pull-in time and pull-in center deflection of microbridge when $C_{vdw} = C_C = C_S = 0$

Applied voltage (V)	Residual stress σ_0 (MPa)							
	100		50		0.0		−15	
	$t_{PI}(t_{ss})$	$w_{PI}^c(w_{ss}^c)$	$t_{PI}(t_{ss})$	$w_{PI}^c(w_{ss}^c)$	$t_{PI}(t_{ss})$	$w_{PI}^c(w_{ss}^c)$	$t_{PI}(t_{ss})$	$w_{PI}^c(w_{ss}^c)$
1.4	(45.8)	(0.033)	(58.1)	(0.054)	(85.20)	(0.163)	39.35	0.539
1.6	(25.0)	(0.043)	(40.1)	(0.072)	(124.10)	(0.255)	11.16	0.460
1.8	(33.5)	(0.056)	(46.7)	(0.095)	37.89	0.481	1.64	0.417
2.0	(38.0)	(0.071)	(77.1)	(0.124)	8.19	0.437	–	–
2.1	(32.3)	(0.079)	(96.9)	(0.141)	2.99	0.420	–	–
2.5	(41.6)	(0.121)	(78.4)	(0.243)	–	–	–	–
3.0	(76.5)	(0.205)	0.83	0.404	–	–	–	–
3.2	(70.9)	(0.262)	–	–	–	–	–	–
3.4	38.4	0.432	–	–	–	–	–	–

the following nondimensional variables are introduced as

$$w = \frac{\hat{w}}{d_0}, \quad x = \frac{\hat{x}}{L}, \quad \text{and} \quad t = \frac{\hat{t}}{T} \tag{32}$$

where T is a time scale and $(\hat{\square})$ denotes a dimensional quantity and d_0 a reference value for the initial gap. For simplicity, we keep the same notations for variables having in mind they are in nondimensional form from now on. Substituting Eq. (32) into Eqs. (29) and (30) and considering no residual stress or axial stretching for microcantilever, the nondimensional governing equation of viscoelastic microbeam can be obtained as

$$\begin{aligned}
 & C_0 \ddot{w}(t) + w''''(t) - C_1 \int_0^t e^{-\bar{\psi}(t-t_0)} w''''(t_0) dt_0 \\
 & - \left[C_R + C_S \int_0^1 w'^2(t) dx \right. \\
 & \left. - C_S \bar{\psi} \bar{E}_2 \int_0^1 \int_0^t e^{-\bar{\psi}(t-t_0)} w'^2(t_0) dt_0 dx \right] w''(t) \\
 & - \frac{C_E}{[1-w(t)]^2} - \frac{C_F}{[1-w(t)]} \\
 & - \frac{C_{vdw}}{[1-w(t)]^3} - \frac{C_C}{[1-w(t)]^4} = 0 \\
 & \forall x \in [0, 1] \text{ and } t \in [t_0, t_f]
 \end{aligned} \tag{33}$$

and the following boundary conditions:

(a) Microcantilever case (Clamped-Free):

$$w(0, t) = w'(0, t) = 0, \tag{34a}$$

$$\begin{aligned}
 & -w'''(1, t) + C_1 \left[\int_0^t e^{-\bar{\psi}(t-t_0)} w'''(1, t_0) dt_0 \right] w'(1, t) = 0 \\
 & \text{and } w''(1, t) - C_1 \int_0^t e^{-\bar{\psi}(t-t_0)} w''(1, t_0) dt_0 = 0
 \end{aligned} \tag{34b}$$

(b) Microbridge case (Clamped–Clamped):

$$w(0, t) = w'(0, t) = 0, \tag{35a}$$

$$w(1, t) = w'(1, t) = 0 \tag{35b}$$

In above equations, the dimensionless parameters are given as follows:

$$\begin{aligned}
 & \Gamma_1 = \Gamma I + \frac{SI^2}{2(1+\nu)}, \quad C_0 = \frac{I}{\Gamma_1}, \quad C_1 = \bar{\psi} \bar{E}_2, \\
 & C_R = \frac{L^2 \sigma_r S}{E_0 \Gamma_1}, \quad C_S = \frac{\Gamma S d_0^2}{\Gamma_1 2}, \\
 & C_E = \frac{I \bar{V}^2}{\Gamma_1}, \quad C_F = 0.65 \frac{d_0}{b} C_e, \quad C_{vdw} = \frac{AbL^4}{6\pi d_0^4 E_0 \Gamma_1}, \\
 & C_C = \frac{\pi^2 \bar{h} c b L^4}{240 d_0^5 E_0 \Gamma_1}, \quad \bar{V} = VL^2 \sqrt{\frac{\varepsilon_0 b}{2d_0^3 E_0 I}}, \\
 & T = \frac{L^2}{h} \sqrt{\frac{12\rho}{E_0}}, \quad \bar{\psi} = \psi T \quad \text{and} \quad \bar{E}_2 = \frac{E_2}{E_0}
 \end{aligned} \tag{36}$$

The parameter is given by Eq. (16). Again, it should be noted that for the case of microcantilevers, the parameters of axial force due to residual stress and

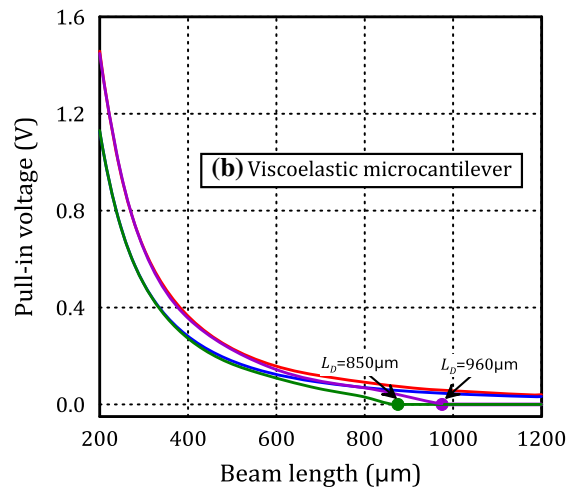
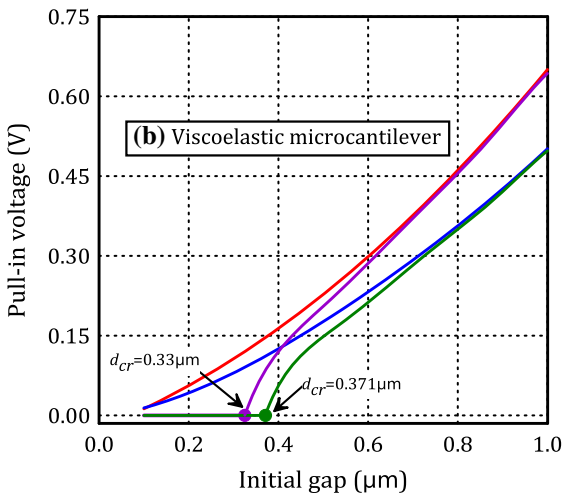
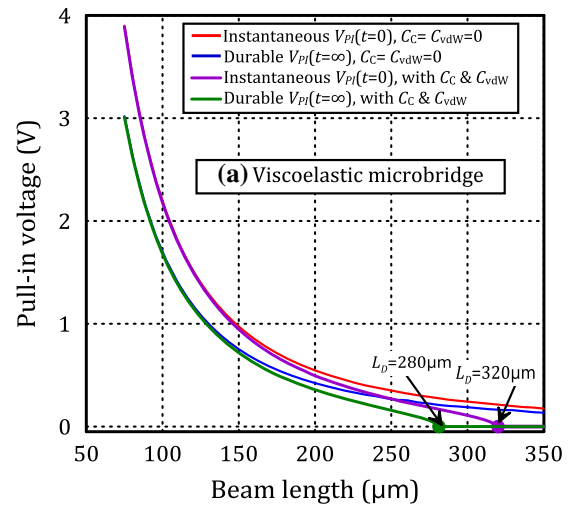
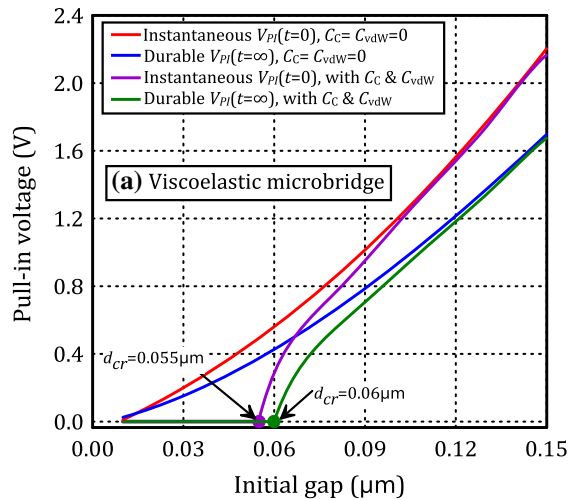


Fig. 7 Effect of the intermolecular Casimir and vdW forces on the instantaneous and durable pull-in voltages at different initial gaps

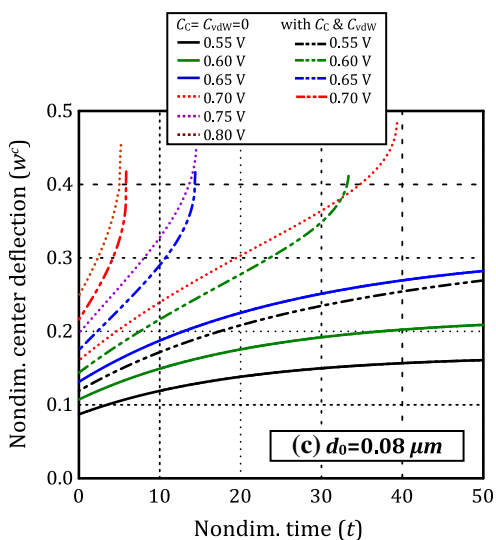
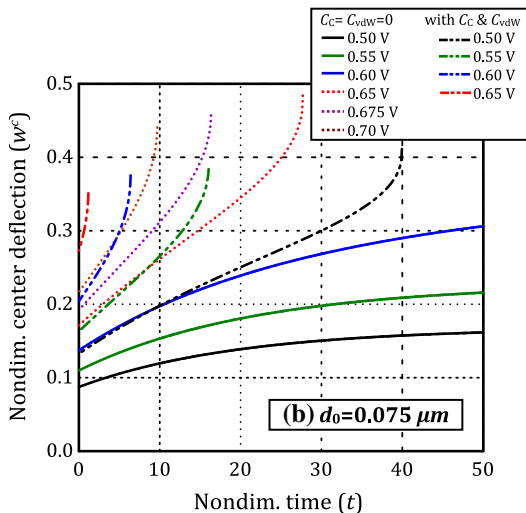
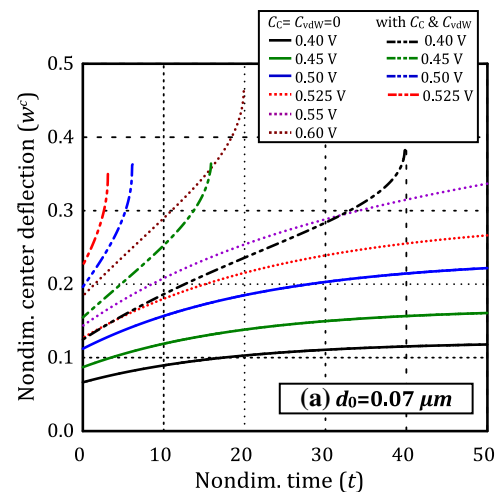
Fig. 8 Effect of the intermolecular Casimir and vdW forces on the instantaneous and durable pull-in voltages at different lengths of the microbeam

nonlinear stretching should be omitted from Eq. (33); i.e. $C_R = C_S = 0$.

3 Solution procedure

Due to the high nonlinearity encountered in the governing equations and associated boundary conditions, analytical solutions for such integro-differential equations is cumbersome. Consequently, an approximate numerical solution is developed through a proposed generalized differential-integral quadrature (GDIQ) method, which is a combination of the well-

known generalized differential quadrature (GDQ) method and a new developed generalized integral quadrature (GIQ) method. In this study, the GDQ method is employed to discretize the governing equation and associated boundary conditions in the space variable. Based on the fact that an indefinite integral of a function is its anti-derivative, a new generalized integral quadrature (GIQ) method is developed as the pseudo-inverse of GDQ method. The proposed GIQ method is applied to approximate the definite integrals included in the integro-differential equation (Eq. (33)). The proposed GDIQ discretization results in a system of ordinary differential equations that can be solved by Runge–Kutta method.



◀ **Fig. 9** Effect of Casimir and vdW forces on the creep of the nondimensional center deflection of viscoelastic microbridge at different initial gaps

3.1 Generalized differential quadrature method

To render the article self-contained, the formulas of the GDQ method, Shu [52] is briefly introduced in this section. The shifted Chebyshev–Gauss–Lobatto grid points are used to generate grid points in x_i direction

$$x_i = \frac{1}{2} \left\{ 1 - \cos \left(\frac{i-1}{N-1} \pi \right) \right\}, \quad i = 1, 2, \dots, N \tag{37}$$

By this method, m -th derivative of a function $f(x, t)$ is discretized by series as follows:

$$\frac{d^m}{dx^m} = \sum_{j=1}^N a_{ij}^{(m)} f(x_j, t) \tag{38}$$

The weighting coefficients $a_{ij}^{(m)}$ for the m -th derivative are dependent on the distribution of grid points only and can be obtained from the recursive formula,

$$a_{ij}^{(m)} = m \left(a_{ij}^{(1)} a_{ii}^{(m-1)} - \frac{a_{ij}^{(m-1)}}{x_i - x_j} \right), \tag{39}$$

$$a_{ii}^{(m)} = - \sum_{j=1, j \neq i}^N a_{ij}^{(m)}, \quad i, j \in \{1, 2, \dots, N\}$$

In matrix form, let the discrete values of $f_i = f(x_i)$ at nodes $i = 1, 2, \dots, N$, be given as a vector $\mathbf{f} = [f_1, f_2, \dots, f_n]^T$, then

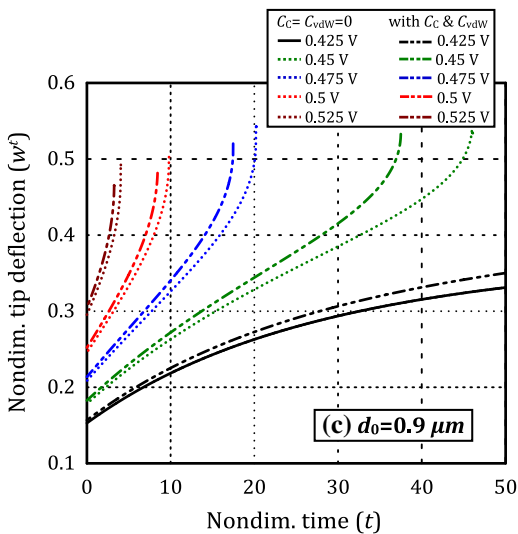
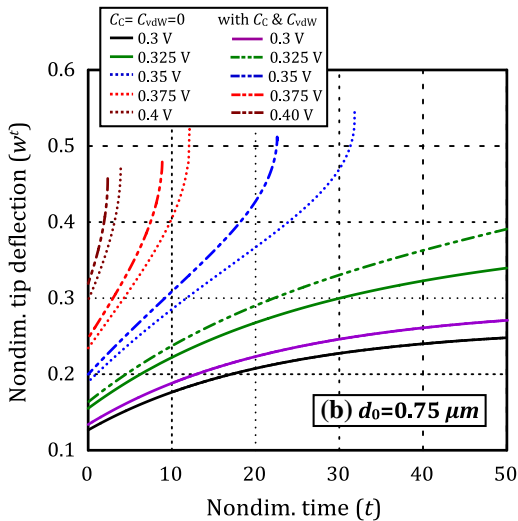
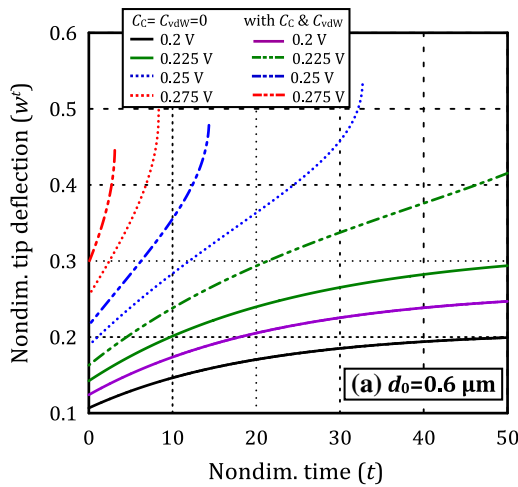
$$\mathbf{F}^{(m)} = \mathbb{A}^{(m)} \mathbf{f} \equiv \mathbb{A}^{(1)} \mathbb{A}^{(m-1)} \mathbf{f} \tag{40}$$

In this work only homogeneous boundary conditions represented by Eqs. (34) and (35) are considered and hence its implementation is straight forward, see Shu [52].

3.2 Generalized integral quadrature method

Consider a differentiable function $f(x)$ defined on the interval $0 \leq x \leq 1$,

$$\frac{df}{dx} = F(x), \quad \int_0^x F(x) dx = f(x) - f(0) \tag{41a, b}$$



◀ **Fig. 10** Effect of Casimir and vdW forces on the creep of the nondimensional tip deflection of viscoelastic microcantilever at different initial gaps

Using a pseudo-inverse algorithm such that the matrix \mathbb{B} is pseudo-inverse of $\mathbb{A}^{(1)}$, one can rewrite Eq. (41a, b) as $\mathbf{f}^{(1)} = \mathbb{B}\mathbf{F}^{(1)}$ and consequently the definite integral between two nodes x_i and x_j can be approximated as

$$\int_{x_i}^{x_j} F(x)dx = f(x_j) - f(x_i) \cong \sum_{k=1}^N \mathbb{R}_{[ij]} F_k, \quad (42)$$

$$k = 1, 2, \dots, N$$

Note that the row vector $\mathbb{R}_{[ij]} = \mathbb{B}_{jk} - \mathbb{B}_{ik}$ is the difference between the j th and i th rows of \mathbb{B} . Thus, the integral $\int_0^1 w'^2 dx$ included in Eq. (33) can be approximated using both GDQ and GIQ methods as follows:

$$\int_0^1 w'^2 dx \cong \mathbb{R}_{[1N]} \left(\left(\mathbb{A}^{(1)} w \right)^{\circ 2} \right), \quad \mathbb{R}_{[ij]} = \mathbb{B}_{jk} - \mathbb{B}_{ik} \quad (43)$$

where the symbol ' \circ ' denotes element by element operator. Note that matrix multiplication of the row $\mathbb{R}_{[1N]}$ by the vector $(\mathbb{A}^{(1)} w)^{\circ 2}$ produces a scalar value approximating the definite integral.

3.3 GDIQ method for viscoelastic analysis

Following Attia and Mohamed [53], the following definitions are firstly introduced:

$$I_1 = \int_0^t e^{-\bar{\psi}(t-t_0)} w''''(t_0) dt_0 \quad (44a)$$

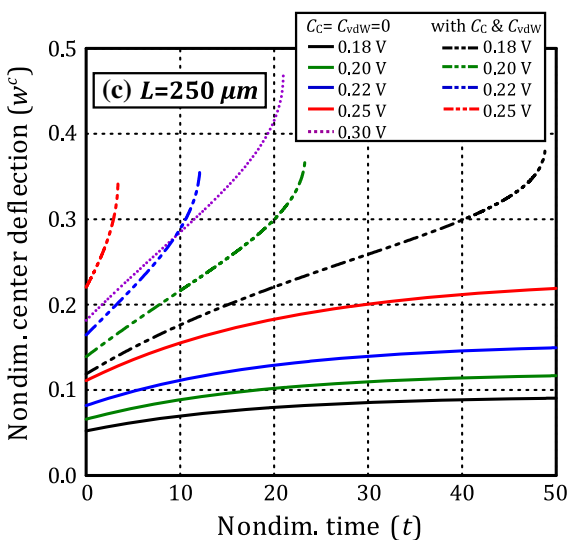
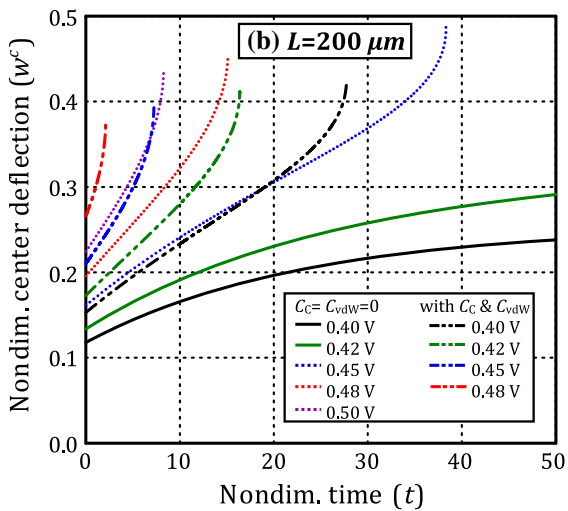
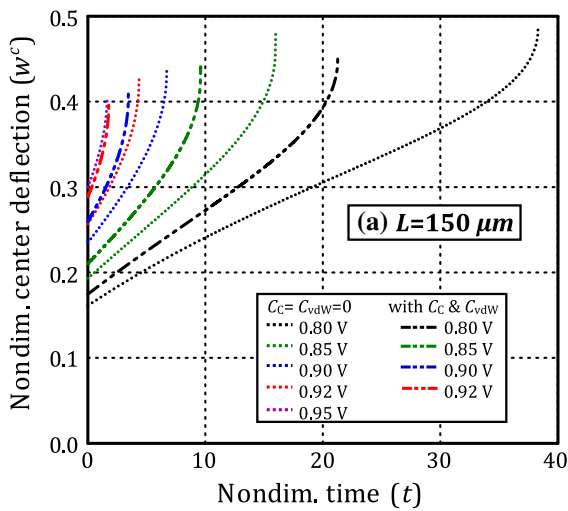
$$I_2 = \int_0^1 \int_0^t e^{-\bar{\psi}(t-t_0)} w'^2(t_0) dt_0 dx \quad (44b)$$

Applying the Leibniz rule for differentiation under the integral sign, one can obtain

$$\dot{I}_1 = w''''(x, t) - \bar{\psi} I_1 \quad \text{and} \quad \dot{I}_2 = g(x, t) - \bar{\psi} I_2 \quad (45a, b)$$

where

$$g(t) = \int_0^1 w'^2(t) dx \quad (46)$$



◀ **Fig. 11** Effect of Casimir and vdW forces on the creep of the nondimensional center deflection of viscoelastic microbridge at different microbeam lengths

Neglecting the inertia term for quasistatic analysis, then differentiation of Eq. (33) with respect to t in light of Eqs. (45a, b) yields to

$$\begin{aligned} & \dot{w}''''(t) - C_1 \dot{I}_1 - [C_R + C_S \{g(t) - \bar{\psi} \bar{E}_2 I_2\}] \dot{w}'' \\ & - C_S \{\dot{g}(t) - \bar{\psi} \bar{E}_2 \dot{I}_2\} w'' \\ & = \left\{ \frac{2C_E}{[1-w]^3} + \frac{C_F}{[1-w]^2} + \frac{3C_{vdW}}{[1-w]^4} + \frac{4C_C}{[1-w]^5} \right\} \dot{w}(t) \\ & \forall x \in [0, 1] \text{ and } t \in [t_i, t_f] \end{aligned} \tag{47}$$

To this end, it is required to reduce Eq. (47) to a system of ODEs using GDQ and GIQ methods. GDIQ method is used to discretize the x -domain and approximate the partial derivatives with respect to x . At arbitrary time t , let $\mathbf{w} = [w_1, w_2, \dots, w_N]^T$ and $\{\dot{\mathbf{w}}\} = [\dot{w}_1, \dot{w}_2, \dots, \dot{w}_N]^T$ be, respectively, the vectors of discrete values of deflection and velocity at the discrete points x_1, x_2, \dots, x_N of the microbeam. Employing the GIQ method defined by Eq. (43) and using Eq. (46), $\dot{g}(t)$ yields to a scalar value as follows

$$\dot{g}(t) = \int_0^1 2w'(x, t) \dot{w}'(x, t) dx = 2\mathbb{R}_{[1N]}((\mathbf{K}_1 \mathbf{w}) \circ (\mathbf{K}_1 \dot{\mathbf{w}})) \tag{48}$$

Consequently, $\dot{g}(t)w''$ can be obtained using GDQ method as follows:

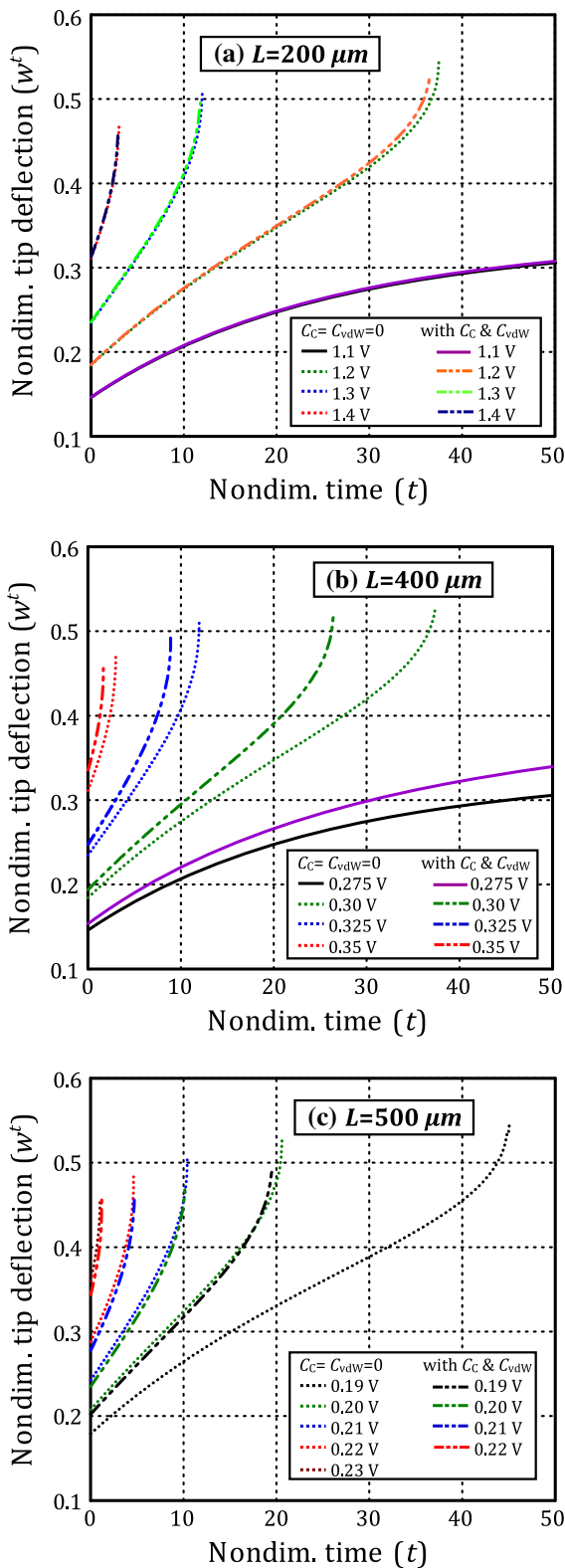
$$\mathbf{K}_2 \mathbf{w} \dot{g}(t) = \mathbf{S} \dot{\mathbf{w}}, \quad \mathbf{S} = 2\mathbf{K}_2 \mathbf{w} \mathbb{R}_{[1N]} \mathbb{Q} \tag{49a, b}$$

where \mathbf{K}_l denotes the coefficients matrix corresponding to the l -th derivatives modified by appropriate application of the boundary conditions. \mathbb{Q} is an N -square matrix obtained from matrix \mathbf{K}_1 by multiplying each element in its i -th row by the corresponding i -th element in vector $\mathbf{w}' = \mathbf{K}_1 \mathbf{w}$. Finally, Eq. (47) can be rewritten

$$\mathbb{M} \dot{\mathbf{w}} = (\mathbf{P} \mathbf{w} - \mathbf{C}) \tag{50}$$

where

$$\begin{aligned} \mathbb{M} = & \mathbf{K}_4 - [C_R + C_S \{g(t) - \bar{\psi} \bar{E}_2 I_2\}] \mathbf{K}_2 - C_S \mathbf{S} \\ & - \left(\frac{2C_E}{[1-w]^3} + \frac{C_F}{[1-w]^2} + \frac{3C_{vdW}}{[1-w]^4} + \frac{4C_C}{[1-w]^5} \right) \end{aligned} \tag{51a}$$



◀ **Fig. 12** Effect of Casimir and vdW forces on the creep of the nondimensional tip deflection of viscoelastic microcantilever at different microbeam lengths

$$\mathbb{P} = C_1 K_4 - \bar{\psi} \bar{E}_2 C_S (g - \bar{\psi} I_2) K_2 \tag{51b}$$

$$\mathbb{C} = \bar{\psi} C_1 I_1 \tag{51c}$$

It is important to refer to that Eqs. (45a, b) and (50) form the coupled system of ODEs obtained from Eq. (47) using GDIQ method. This system is solved using Runge–Kutta method. However, the initial conditions have to be computed first by substituting $t = 0$ into Eq. (33),

$$w'''' - \left[C_R + C_S \int_0^1 w'^2 dx \right] w'' - \frac{C_E}{[1-w]^2} - \frac{C_F}{[1-w]} - \frac{C_{vdW}}{[1-w]^3} - \frac{C_C}{[1-w]^4} = 0 \quad \forall x \in [0, 1] \tag{52}$$

which can be solved using Newton’s iterative method to obtain w_0 .

4 Numerical results and discussion

In this section, the proposed model is verified by comparing the obtained results with those of available numerical and analytical methods in the literature. Also, a comprehensive parametric study is conducted to investigate the different viscoelastic material and geometrical parameters as well as the intermolecular forces on the quasistatic pull-in response of electrically actuated viscoelastic doubly-clamped microbridges and clamped-free microcantilevers in the framework of viscoelasticity.

4.1 Comparative study

Since, there is no available well-defined benchmarks to validate the present model for electrically actuated viscoelastic microbeams including the combined effects of length scale parameter, fringing field, residual stresses, mid-plane stretching and Casimir and vdW forces. Therefore, based on the

Table 4 Effect of the Casimir and vdW forces on the nondimensional pull-in time and pull-in maximum deflection

Initial gap $d_0(\mu\text{m})$	Applied voltage (V)	Intermolecular forces							
		$C_C = C_{\text{vdW}} = 0$		with C_C ($C_{\text{vdW}} = 0$)		with C_{vdW} ($C_C = 0$)		with C_C and C_{vdW}	
		$t_{PI}(t_{ss})$	$w_{PI}(w_{ss})$	$t_{PI}(t_{ss})$	$w_{PI}(w_{ss})$	$t_{PI}(t_{ss})$	$w_{PI}(w_{ss})$	$t_{PI}(t_{ss})$	$w_{PI}(w_{ss})$
Viscoelastic microbridge, $w_{PI}^c(w_{ss}^c)$									
0.07	0.4	(20.2)	(0.122)	(158.3)	(0.240)	(91.2)	(0.163)	39.85	0.382
	0.45	(99.5)	(0.167)	43.75	0.390	(112.4)	(0.225)	15.85	0.364
	0.5	(122.4)	(0.235)	15.6	0.386	123.2	0.473	6.15	0.363
	0.525	(144.6)	(0.291)	9.5	0.377	41.45	0.461	3.1	0.350
	0.55	105.95	0.496	5.4	0.366	22.75	0.462	0.856	0.337
	0.6	19.9	0.462	0.21	0.348	7.75	0.437	–	–
	0.65	5.94	0.437	–	–	0.982	0.388	–	–
0.075	0.5	(103.7)	(0.168)	(195.6)	(0.298)	(131)	(0.210)	39.95	0.411
	0.55	(121.3)	(0.228)	33.5	0.407	(182.9)	(0.307)	16.05	0.384
	0.6	(281.8)	(0.371)	13.1	0.389	36.55	0.477	6.4	0.375
	0.65	27.7	0.484	4.55	0.383	13.15	0.429	1.17	0.351
	0.675	16.35	0.457	1.915	0.371	7.86	0.422	–	–
	0.7	9.7	0.440	–	–	4.17	0.408	–	–
	0.75	2.23	0.421	–	–	–	–	–	–
0.08	0.55	(93.5)	(0.167)	(121)	(0.234)	(108.4)	(0.198)	242.45	0.431
	0.6	(113.5)	(0.220)	83.3	0.449	(145.6)	(0.269)	33.35	0.412
	0.65	(165.3)	(0.315)	24.8	0.444	63.05	0.479	14.4	0.417
	0.7	39.35	0.483	10.4	0.391	20.8	0.482	5.85	0.417
	0.75	14.5	0.447	3.65	0.426	8.2	0.415	1.08	0.368
	0.8	5.2	0.453	0.37	0.312	2.12	0.409	–	–
	0.82	2.82	0.411	–	–	–	–	–	–
Viscoelastic microcantilever, $w_{PI}^t(w_{ss}^t)$									
0.60	0.2	(137.8)	(0.208)	(133.8)	(0.217)	(108.2)	(0.249)	(116.5)	(0.262)
	0.225	(148.2)	(0.318)	(190.6)	(0.343)	97.75	0.537	61.55	0.524
	0.25	32.7	0.532	26.4	0.530	17.3	0.503	14.35	0.479
	0.275	8.35	0.498	6.9	0.486	4.09	0.458	3.1	0.446
	0.75	0.3	(133.1)	(0.262)	(121.9)	(0.266)	(183.4)	(0.285)	(145.2)
0.325		(191.1)	(0.393)	(356.1)	(0.427)	99	0.555	81.8	0.536
0.35		31.83	0.544	29.58	0.535	24.13	0.513	22.59	0.507
0.375		12.12	0.522	11.4	0.539	9.5	0.524	8.85	0.479
0.4		3.89	0.470	3.55	0.465	2.62	0.469	2.335	0.457
0.9		0.425	(173.7)	(0.375)	(177.7)	(0.381)	(453.3)	(0.430)	337.3
	0.45	46.1	0.534	44.27	0.534	38.79	0.535	37.5	0.533
	0.475	20.25	0.542	19.8	0.535	17.93	0.519	17.47	0.520
	0.5	9.81	0.503	9.55	0.490	8.68	0.483	8.47	0.519
	0.525	4.055	0.492	3.905	0.477	3.39	0.471	3.26	0.465
	0.55	0.493	0.448	0.413	0.451	–	–	–	–

Table 5 Effect of the Casimir and vdW forces on the nondimensional pull-in time and pull-in maximum deflection

Beam length $L(\mu\text{m})$	Applied voltage (V)	Intermolecular forces								
		$C_C = C_{\text{vdW}} = 0$		with C_C ($C_{\text{vdW}} = 0$)		with C_{vdW} ($C_C = 0$)		with C_C & C_{vdW}		
		$t_{PI}(t_{ss})$	$w_{PI}(w_{ss})$	$t_{PI}(t_{ss})$	$w_{PI}(w_{ss})$	$t_{PI}(t_{ss})$	$w_{PI}(w_{ss})$	$t_{PI}(t_{ss})$	$w_{PI}(w_{ss})$	
<i>Viscoelastic microbridge, $w_{PI}^c(w_{ss}^c)$</i>										
150	0.8	38.32	0.489	27.18	0.468	28.86	0.462	21.27	0.454	
	0.85	16.01	0.479	12.06	0.436	12.73	0.451	9.61	0.439	
	0.9	6.71	0.440	4.76	0.445	5.09	0.421	3.46	0.412	
	0.92	4.36	0.428	2.81	0.404	3.07	0.407	1.78	0.396	
	0.95	1.645	0.406	0.575	0.388	0.765	0.421	–	–	
200	0.4	(118.8)	(0.254)	84.8	0.465	148.8	0.487	27.72	0.422	
	0.42	(190)	(0.331)	34.96	0.457	42.41	0.466	16.39	0.410	
	0.45	38.32	0.489	14.81	0.418	17.18	0.450	7.24	0.393	
	0.48	15.12	0.453	6.08	0.397	7.22	0.427	2.1	0.375	
	0.5	8.27	0.435	2.58	0.383	3.33	0.411	–	–	
250	0.52	3.9	0.424	0.165	0.376	0.647	0.390	–	–	
	0.18	(78)	(0.093)	(93.6)	(0.160)	(98.9)	(0.166)	48.82	0.380	
	0.2	(75.6)	(0.120)	(138.6)	(0.209)	(132.2)	(0.211)	23.26	0.367	
	0.22	(95.6)	(0.155)	162.85	0.419	(201.1)	(0.291)	12.09	0.359	
	0.25	(140.22)	(0.232)	21.72	0.395	29.25	0.437	3.375	0.341	
250	0.3	20.98	0.468	1.48	0.362	2.8	0.384	–	–	
	0.32	8.31	0.448	–	–	–	–	–	–	
	<i>Viscoelastic microcantilever, $w_{PI}^t(w_{ss}^t)$</i>									
	200	1.1	(144)	(0.334)	(170.8)	0.3350	(170.9)	0.337	(152)	(0.337)
		1.2	37.5	0.544	37.3	0.546	36.7	0.563	36.5	0.528
1.3		12	0.510	11.9	0.494	11.8	0.510	11.8	0.496	
1.4		3.05	0.472	3	0.476	2.95	0.467	2.9	0.457	
400	0.275	(143.9)	(0.334)	(200)	0.341	(228.8)	0.388	(320.6)	(0.408)	
	0.3	37.4	0.530	35.2	0.526	27.8	0.527	26.4	0.516	
	0.325	11.98	0.507	11.41	0.497	9.37	0.539	8.9	0.495	
500	0.35	2.99	0.469	2.75	0.459	1.845	0.454	1.66	0.456	
	0.19	45.1	0.548	38.3	0.565	21.85	0.501	19.5	0.489	
	0.2	20.6	0.528	18.3	0.499	11.4	0.480	10.15	0.468	
	0.21	10.41	0.503	9.27	0.498	5.42	0.472	4.7	0.456	
	0.22	4.63	0.485	3.93	0.454	1.62	0.452	1.2	0.458	
	0.23	1.015	0.456	0.615	0.446	–	–	–	–	

quasi-elastic method proposed by Schapery [54], the current results of the nondimensional instantaneous and durable pull-in voltages (\bar{V}_{PI}) at times $t = 0$ and ∞ , respectively, of a doubly-clamped microbridge viscoelastic microactuator are compared with those reported by Zhang and Fu [41], in which $E_0 = 169$ GPa, $\bar{E}_1 = 0.6$, $\nu = 0.22$, $L = 150 \mu\text{m}$, $b = 10 \mu\text{m}$, $h = 2 \mu\text{m}$ and $d_0 = 1.2h$. For the purpose

of comparison, the effects of the fringing field, residual stresses and Casimir and vdW forces are neglected; i.e. $C_F = C_R = C_C = C_{\text{vdW}} = 0$, while the effect of mid-plane stretching is included. As shown in Fig. 2, it is found that the present results are in good agreement with those in the work of Zhang and Fu [41] for different values of nondimensional length scale parameter l/h .

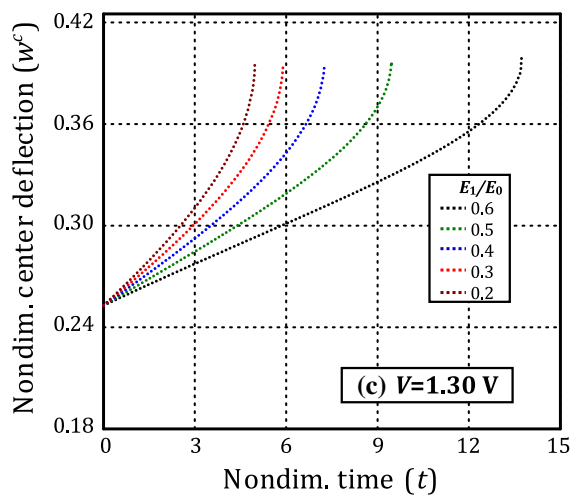
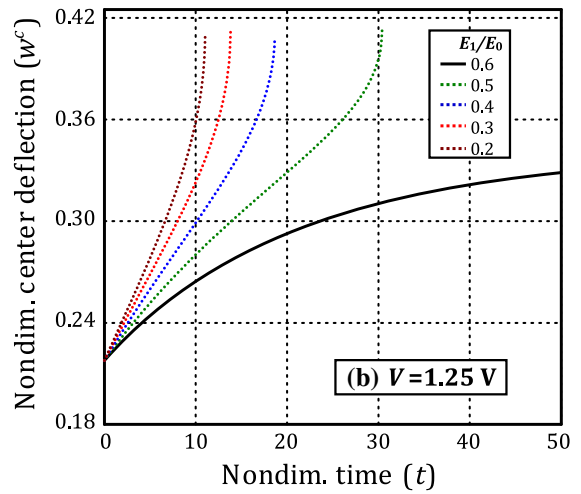
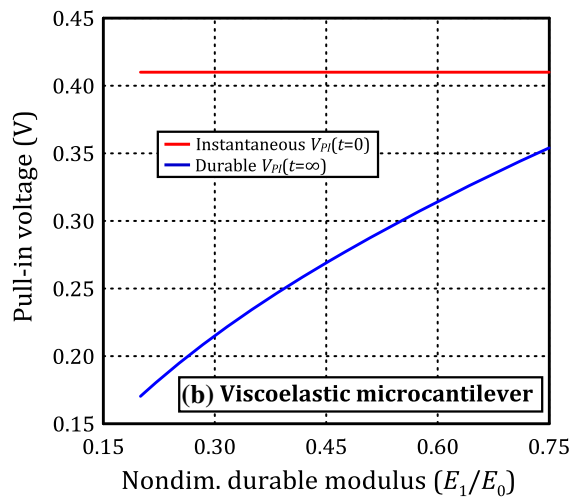
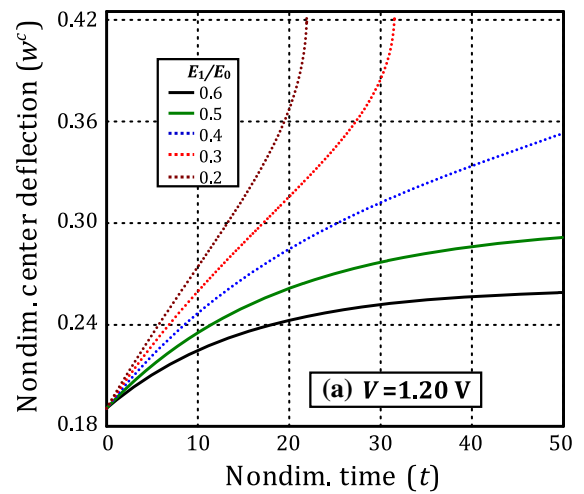
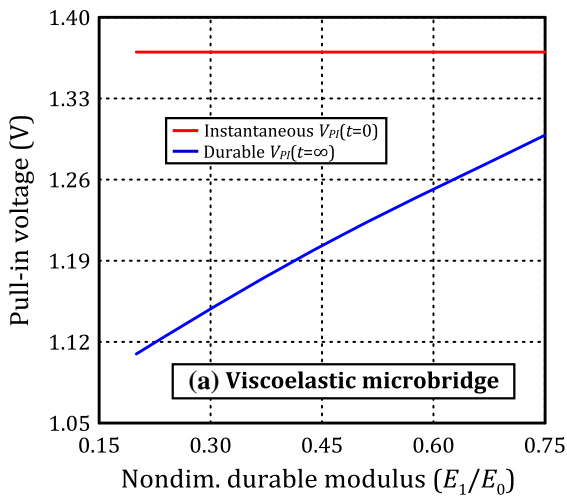


Fig. 13 Effect of the nondimensional durable modulus \bar{E}_1 on the viscoelastic instantaneous and durable pull-in voltages

Also, convergence of the present numerical method is verified as demonstrated in Table 1 which displays and compares the linear (without mid-plane stretching) and nonlinear (with mid-plane stretching) pull-in voltages of elastic microbridge of different lengths with varying total number of grid points N . As observed, the proposed numerical GDIQ method yields convergent results when $N \geq 21$. Moreover, it is seen from Table 1 that the present results are in a good agreement with those obtained using numerical, analytical and experimental methods. Based on these results, all the following numerical results are obtained using $N = 21$.

◀ **Fig. 14** Effect of the nondimensional durable modulus \bar{E}_1 on the creep of the nondimensional center deflection of viscoelastic microbridge

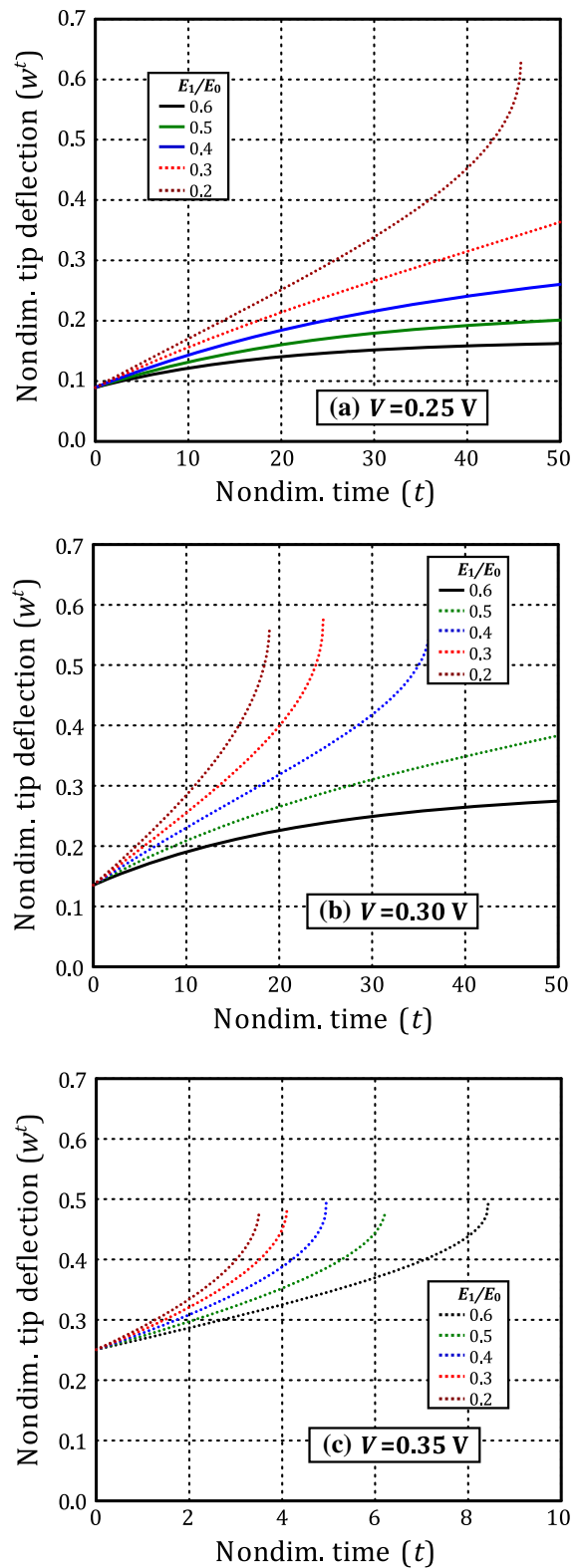
4.2 Parametric study

The developed model is used to investigate the nonlinear size-dependent quasistatic pull-in response of electrically actuated viscoelastic microbridges and microcantilevers based on the MCST. Combined effect of electrostatic actuation, fringing field, mid-plane stretching, residual stresses and Casimir and vdW forces are considered. Effect of mid-plane stretching, residual stresses, initial gap, beam length, Casimir force, vdW force, durable modulus, relaxation time, and material length scale parameter on the viscoelastic pull-in parameters; i.e. instantaneous and durable pull-in voltages, viscoelastic creep deflection, pull-in time and pull-in deflection, will be comprehensively studied in the next sections.

Material parameters of both doubly-clamped microbridge and clamped-free microcantilever are $E_0 = 77$ GPa, $\bar{E}_1 = 0.6$, $\bar{\psi} = 0.1$, $\nu = 0.33$, $l = 0.25h$ and the residual stress σ_0 is taken 100 MPa for the case of doubly-clamped microbeam. Geometrical parameters are taken as $L = 100 \mu\text{m}$, $b = 50 \mu\text{m}$, $h = 1 \mu\text{m}$ and $d_0 = 0.08 \mu\text{m}$ for the microbridge and $L = 300 \mu\text{m}$, $b = 50 \mu\text{m}$, $h = 1 \mu\text{m}$ and $d_0 = 0.15 \mu\text{m}$ for the microcantilever. These material and geometrical parameters are hold constant except the parameter being studied, which is varied with larger or smaller value.

4.2.1 Effect of mid-plane stretching

It is worth noting that for the geometrical nonlinearity caused by mid-plane stretching to be significant, the beam ends must be immovable, Nayfeh and Mook [55]. Also, it is noticed from Eq. (36) that this source of nonlinearity is proportional to the square of the initial gap. The effect of mid-plane stretching on the instantaneous and durable pull-in voltages of the doubly-clamped microbridge for different initial gaps is presented in Fig. 3, using the quasi-elastic analysis. The results are obtained corresponding to both linear and nonlinear analyses based on the MCST for $l/h = 0.25$ and ignoring the effects fringing field, residual



◀ **Fig. 15** Effect of the nondimensional durable modulus \bar{E}_1 on the creep of the nondimensional tip deflection of viscoelastic microcantilever

stresses and intermolecular Casimir and vdW forces; i.e. $C_F = C_R = C_{vdW} = C_C = 0$. According to these results, it is observed that as the initial gap increases, the instantaneous and durable pull-in voltages for both linear (without mid-plane stretching effect “ $C_S = 0$ ”) and nonlinear (with mid-plane stretching effect “with C_S ”) responses are significantly increased. Also, it is revealed that the nonlinear pull-in voltage is larger than that obtained from linear analysis and therefore ignoring nonlinearity due to mid-plane stretching leads to underestimation of both instantaneous and durable pull-in voltages especially at large initial gaps.

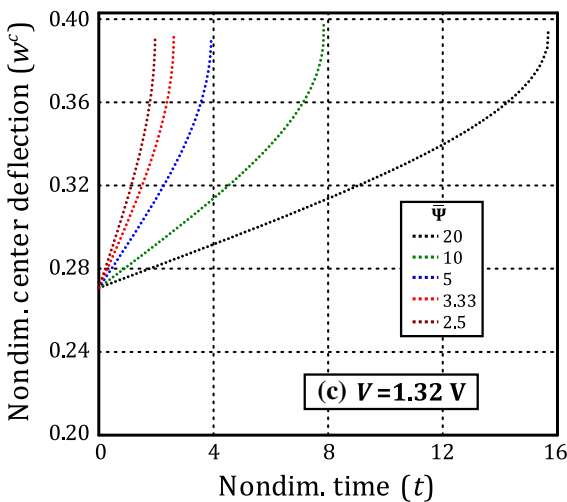
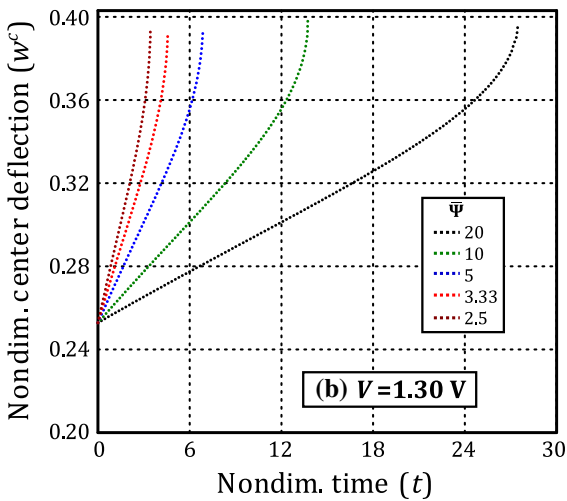
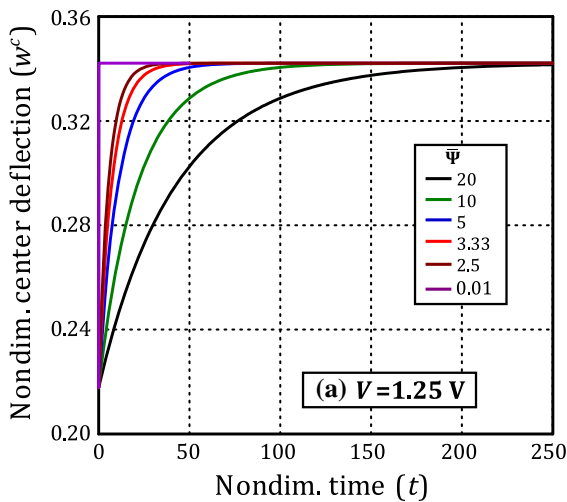
Creep of the linear and nonlinear nondimensional center deflection for different initial gaps and applied voltages is studied in Fig. 4. Here and throughout the paper, the solid line denote that the microactuator behaves stable when the applied voltage is lower than the durable one ($V < V_{PI}(t = \infty)$), i.e. the microactuated beam will not collapse at any time instant. Both dash and dash-dot lines represent that the microactuator behaves in the durable region when $V_{PI}(t = \infty) < V < V_{PI}(t = 0)$. Some selected numerical values for the nondimensional pull-in time (t_{PI}) and the corresponding nondimensional pull-in center deflection of microbridge (w_{PI}^c) are provided in

Table 2. This Table and next tables throughout the paper can be recognized to three different regions according to the status of the microactuator response; namely stable, durable, and invisible regions. The *stable region*, where the beam will not collapse any time, is identified by nondimensional time elapsed by the microbeam to reach the steady-state response (t_{ss}) and corresponding nondimensional steady-state center deflection (w_{ss}^c), which appear with parentheses. The *durable region* reports the values of the nondimensional pull-in time (t_{PI}) and the corresponding nondimensional pull-in center deflection (w_{PI}^c) just before collapse. The third region presents the *unstable or invisible one*, which is filled by the symbol “–”, to indicate that no response exists. Noting that instantaneous pull-in (at no time) occurs in the transition between the durable and invisible regions ($V > V_{PI}(t = 0)$), while the durable pull-in occurs between the durable and stable regions.

From the results presented in Fig. 4 and Table 2, it is noticed that the difference between linear and nonlinear responses of viscoelastic microbridge becomes more significant at large values of the initial gap. Also, at large initial gaps, including the nonlinear mid-plane stretching effect may drive the microbridge to behave in the durable region instead of the unstable one. It is also detected that for large initial gaps and applied voltages, the nondimensional pull-in time and nondimensional pull-in center deflection are

Table 6 Effect of the nondimensional durable modulus \bar{E}_1 on the nondimensional pull-in time and pull-in maximum deflection

Applied voltage (V)	Nondimensional durable modulus $\bar{E}_1 = E_1/E_0$									
	0.6		0.5		0.4		0.3		0.2	
	$t_{PI}(t_{ss})$	$w_{PI}(w_{ss})$	$t_{PI}(t_{ss})$	$w_{PI}(w_{ss})$	$t_{PI}(t_{ss})$	$w_{PI}(w_{ss})$	$t_{PI}(t_{ss})$	$w_{PI}(w_{ss})$	$t_{PI}(t_{ss})$	$w_{PI}(w_{ss})$
Viscoelastic microbridge, $w_{PI}^c(w_{ss}^c)$										
1.1	(58.3)	(0.191)	(69.4)	(0.207)	(99.6)	(0.228)	(111.8)	(0.257)	(271.1)	(0.314)
1.2	(95.61)	(0.262)	(117.9)	(0.300)	68.55	0.412	31.54	0.424	21.92	0.417
1.25	(121.4)	(0.342)	30.4	0.413	18.65	0.408	13.81	0.412	11.02	0.409
1.3	13.75	0.400	9.47	0.394	7.25	0.395	5.9	0.394	4.97	0.397
1.35	2.515	0.390	1.955	0.383	1.605	0.389	1.36	0.388	1.18	0.390
Viscoelastic microcantilever, $w_{PI}^t(w_{ss}^t)$										
0.25	(95.6)	(0.168)	(223.6)	(0.220)	(322.2)	0.348)	77.6	0.639	45.8	0.633
0.3	(199)	(0.295)	80.05	0.581	36.3	0.563	24.8	0.578	18.95	0.559
0.35	21.64	0.518	14.03	0.508	10.51	0.532	8.44	0.538	7.03	0.509
0.375	8.45	0.488	6.23	0.481	4.96	0.497	4.1	0.482	3.51	0.477



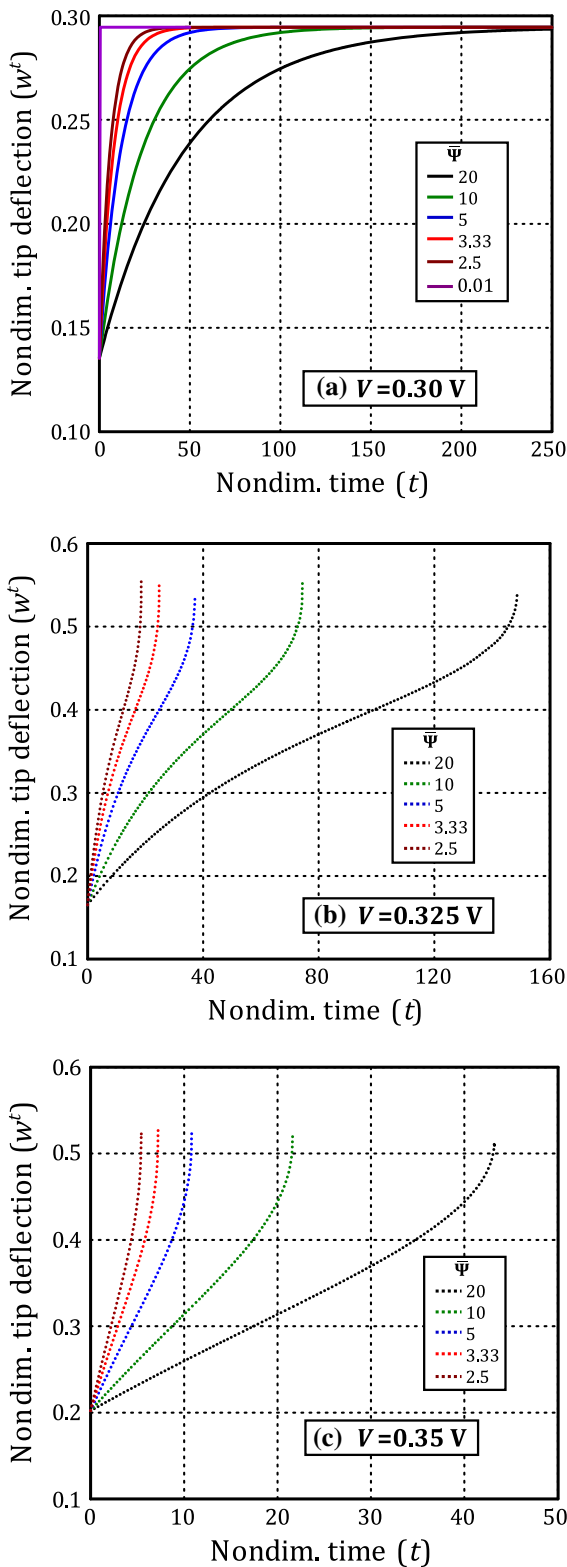
◀ **Fig. 16** Effect of the nondimensional relaxation time $\bar{\Psi}$ on the creep of the nondimensional center deflection of viscoelastic microbridge

underestimated while the nondimensional instantaneous center deflection (at $t = 0$) is overestimated when the mid-plane stretching effect is neglected, i.e. $d_0 = 1 \mu\text{m}$. If the microbridge behaves in the stable region for both linear and nonlinear analysis ($d_0 = 1 \mu\text{m}$ and $V = 29\text{V}$), a remarkable decrease in the nondimensional steady-state time and nondimensional steady-state deflection is obtained when the mid-plane stretching is considered.

4.2.2 Effect of residual stresses

Depending on the fabrication sequences of the MEM actuators, the residual stresses can be tensile or compression, Kahn and Heuer [56]. Figure 5 illustrates the variation of the instantaneous and durable pull-in voltages of viscoelastic microbridge with the residual stress considering the fringing field effect when $d = 0.15 \mu\text{m}$, $l/h = 0.25$ and $C_{vdw} = C_C = C_S = 0$. It is clear that increasing the residual stress from compressive towards tensile direction results in a significant increase in both instantaneous and durable pull-in voltages of the microbridge. Consequently the size of the stable region is increased, whilst the sizes of the durable and unstable regions are decreased. This is because that the tensile residual stress stiffens microbridges but conversely compressive residual stress softens them. Also, it is worth noting that varying the compressive residual stress has a more pronounced influence on the pull-in voltages rather than varying the tensile residual stress. As the residual stress is varied from -3.2 to -20MPa , the instantaneous and durable pull-in voltages are decreased by 18.18 and 35.09% respectively. Changing the residual stress from 4 to 20.8 MPa shows a 13.22 and 20.61% increase in the instantaneous and durable pull-in voltages, respectively.

Effect of the residual stress on the creep of the nondimensional center deflection of viscoelastic microbridge is shown in Fig. 6 and selected values of the nondimensional pull-in time and pull-in center deflection for various residual stresses are provided in Table 3. It is clear that as the tensile residual stress is



◀ **Fig. 17** Effect of the nondimensional relaxation time $\bar{\Psi}$ on the creep of the nondimensional tip deflection of viscoelastic microcantilever

increased, the nondimensional steady-state (durable) center deflection and time required to reach it are significantly decreased; this response is represented by the solid lines in Fig. 6 and the values appear with parentheses in Table 3. From the obtained results, it is noticed that compressive residual stress shows a distinct increase in the nondimensional instantaneous center deflection, while the nondimensional pull-in time and corresponding nondimensional pull-in center deflection are obviously decreased. In other words, compressive residual stress makes the microbridge state to be converted from the stable region to the durable or invisible one.

4.2.3 Effect of Casimir and vdW forces

Since the intermolecular forces are the spontaneous attractive forces between the flexible beam and the fixed substrate, the flexible beam will attach the fixed substrate even without an electrostatic attraction if the intermolecular Casimir and vdW forces reach certain critical values. It is clear from Eq. (36) that the Casimir and vdW parameters, C_C and C_{vdW} are inversely proportional to, respectively, the fourth and fifth power of the initial gap and both C_C and C_{vdW} are directly proportional to the fourth power of the beam length. Consequently, this section is intended to explore the effects of the intermolecular Casimir and vdW forces on the size-dependent pull-in stability by considering the following two case studies: (1) varying the initial gap d_0 while keeping other material and geometrical parameters as constants and (2) varying the beam length L while holding other material and geometrical parameters as constants. For both cases, the results are obtained for both viscoelastic microbridge and microcantilever with and without the effects of Casimir and vdW forces at $l = 0.25h$ when the fringing field, mid-plane stretching and residual stress are neglected; i.e. $C_F = C_S = C_R = 0$.

Effect of the intermolecular Casimir and vdW forces on the instantaneous and durable pull-in voltages of viscoelastic microbridge and microcantilever is plotted in Fig. 7 for different values of the

Table 7 Effect of the nondimensional relaxation coefficient $\bar{\Psi}$ on the nondimensional pull-in time and pull-in maximum deflection

Applied voltage (V)	Nondimensional durable modulus $\bar{\Psi} = 1/\Psi$									
	20		10		5		3.33		2.5	
	$t_{PI}(t_{ss})$	$w_{PI}(w_{ss})$	$t_{PI}(t_{ss})$	$w_{PI}(w_{ss})$	$t_{PI}(t_{ss})$	$w_{PI}(w_{ss})$	$t_{PI}(t_{ss})$	$w_{PI}(w_{ss})$	$t_{PI}(t_{ss})$	$w_{PI}(w_{ss})$
Doubly-clamped microactuator, $w_{PI}^c(w_{ss}^c)$										
1.25 V	(244.2)	(0.342)	(121.4)	(0.342)	(60.6)	(0.342)	(40.4)	(0.342)	(30.4)	(0.342)
1.28	49.15	0.399	24.64	0.408	12.3	0.402	8.21	0.404	6.15	0.401
1.3	27.46	0.395	13.75	0.400	6.87	0.394	4.58	0.403	3.43	0.394
1.32	15.7	0.394	7.845	0.399	3.92	0.390	2.64	0.405	1.96	0.390
1.35	5.015	0.388	2.515	0.390	1.26	0.387	0.845	0.397	0.625	0.380
Cantilever microactuator, $w_{PI}^t(w_{ss}^t)$										
0.3 V	(244.6)	(0.294)	(199)	(0.295)	(99.4)	0.295	(66.4)	(0.295)	(50)	(0.295)
0.325	148.68	0.540	74.41	0.554	37.11	0.540	24.77	0.538	18.56	0.530
0.35	43.23	0.504	21.64	0.518	10.81	0.523	7.22	0.529	5.43	0.518
0.375	16.9	0.504	8.45	0.488	4.21	0.493	2.810	0.492	2.11	0.494

initial gap and Fig. 8 for various values of the beam length. As seen in Fig. 7, the instantaneous and durable pull-in voltages for both viscoelastic microbridge and microcantilever are decreased as the initial gap decreases. For a specific beam length, the difference between the critical initial gaps (d_{cr}) with and without considering intermolecular Casimir and vdW forces indicates the intermolecular forces significantly affect the value of the critical initial gap. Also, at small values of the initial gap ($d \leq d_{cr}$), Casimir and vdW forces drive the microactuator to be collapsed at no time without applied voltage. It is evident in Fig. 8 that for both microbridge and microcantilever, increasing length of the microactuators results in a decrease in the instantaneous and durable pull-in voltages and consequently the region of stable response is decreased. For a constant initial gap, the maximum beam length such that the collapse will occur at no time at lengths just larger than it ($L \geq L_D$) in the absence of applied voltage, is known as the detachment length L_D . It is clear that including the Casimir and vdW forces shows a remarkable decrease in the detachment length for both microbridge and microcantilever.

Moreover, it is detected that for viscoelastic microbridge and microcantilever, including the Casimir and vdW forces results in a noticeable decrease in the instantaneous and durable pull-in voltages. Also, it is observed that for large values of the initial gap or small values of the microactuator length, the pull-in

voltage obtained with and without Casimir and vdW forces are identical. Comparing Fig. 7 with 8, it is found that the effect of decreasing the initial gap on the contribution of Casimir and vdW forces is more noticeable than that of increasing the microactuator length. Additionally, one can find that the effects of the initial gap and beam length are more pronounced for doubly-clamped microbridge.

Creep of the nondimensional pull-in center and tip deflections of the viscoelastic microbridge and microcantilever with and without the effect of Casimir and vdW forces is illustrated in Figs. 9–12. Figures 9 and 10 present the results for various initial gaps and Figs. 11 and 12 correspond to different values of beam length. Selected numerical values for the nondimensional pull-in time and corresponding nondimensional pull-in deflections with and without Casimir and vdW forces are provided in Tables 4 and 5 for various values of the initial gap and beam length, respectively.

According to the obtained results, for the same applied voltage, accounting for the intermolecular Casimir and vdW forces shows an increase in the nondimensional instantaneous deflection and a decrease in the nondimensional pull-in deflection, especially at small gap values or large lengths of the microactuator. This remark is for both viscoelastic microbridge and microcantilever.

At low applied voltages, the state of the beam lies in the stable region without and with the influence of

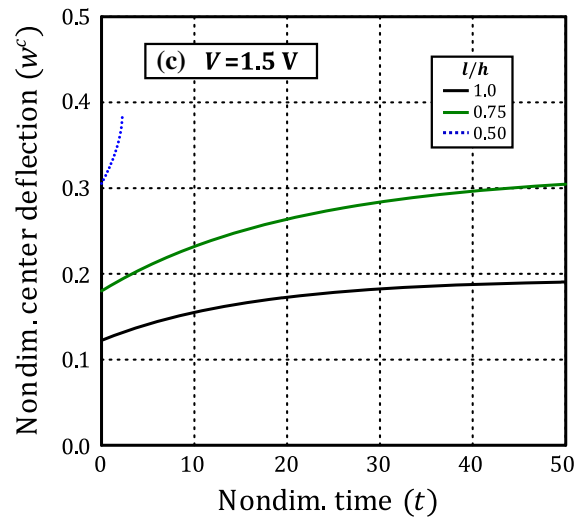
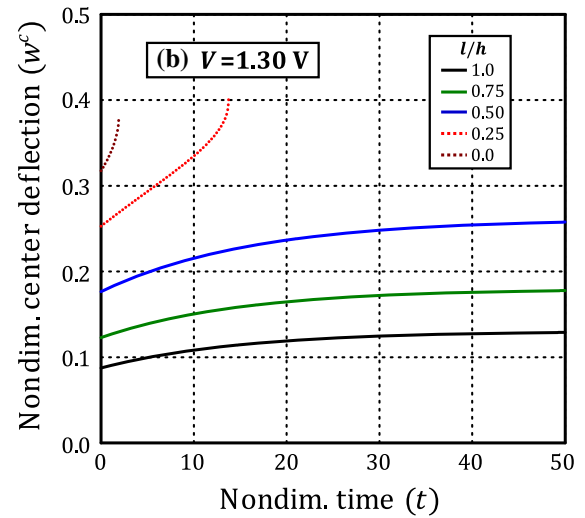
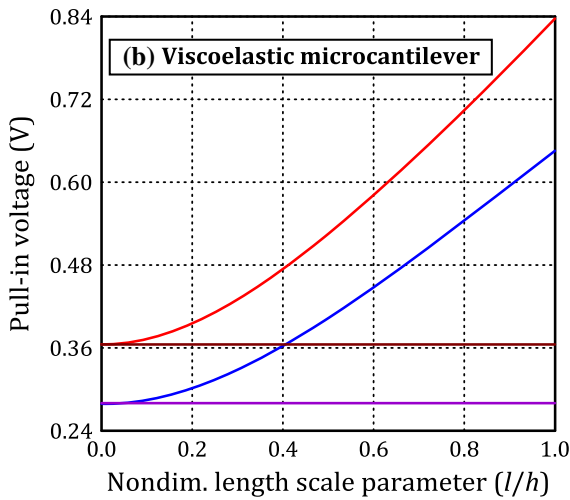
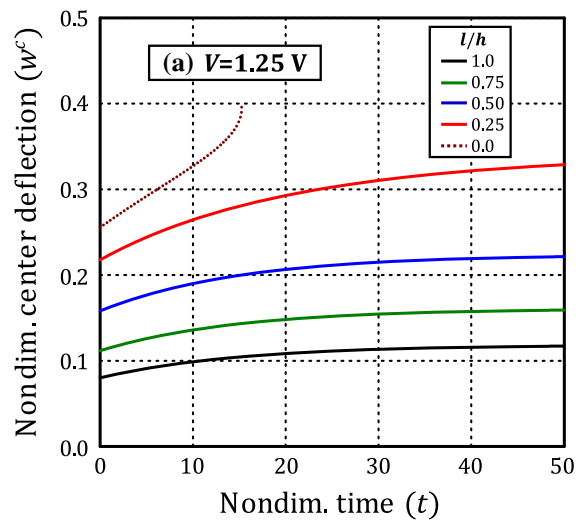
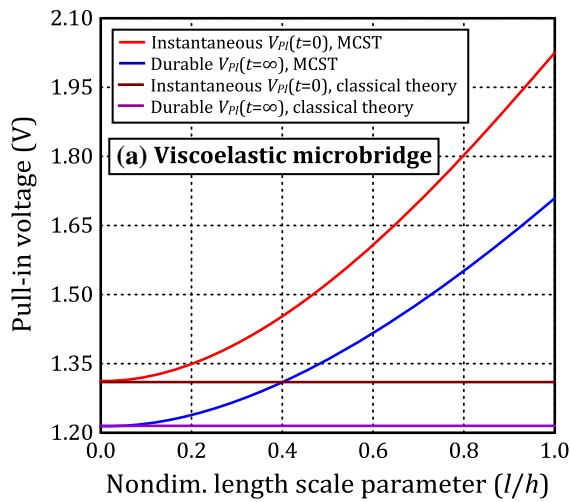


Fig. 18 Effect of the nondimensional material length scale parameter l/h on the viscoelastic instantaneous and durable pull-in voltages

Casimir or vdW forces (solid lines in Figs. 9–12 and values with parentheses in Tables 4 and 5) and both the viscoelastic instantaneous and durable (steady-state) deflections are significantly increased. However, the combined influence of Casimir and vdW forces may tend the microbeam to behave in the durable or invisible region instead of stable one and a remarkable increase in the instantaneous and pull-in deflections are detected. In the durable region, it is noted that the individual or combined effect of Casimir and vdW forces leads to a distinct decrease in the nondimensional pull-in time and nondimensional pull-in deflection. Consequently, ignoring the individual or combined effect of Casimir and vdW forces may lead

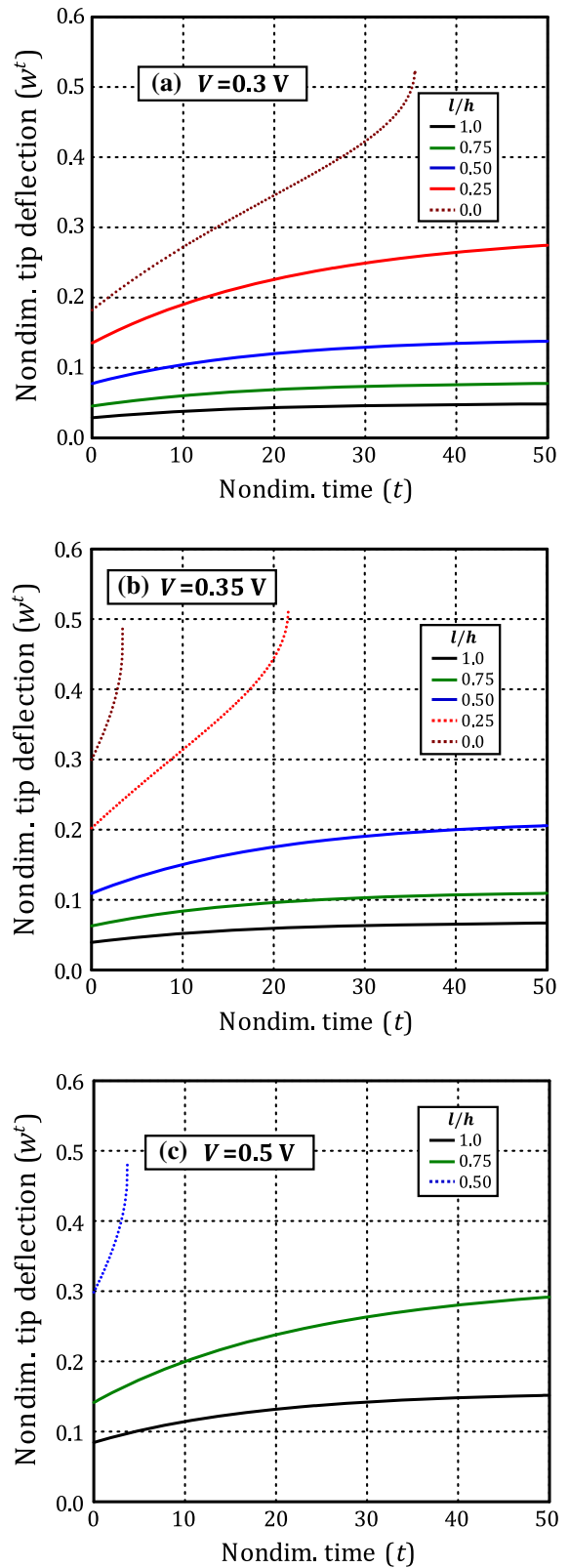
◀ **Fig. 19** Effect of the nondimensional material length scale parameter l/h on the creep of the nondimensional center deflection of viscoelastic microbridge

to considerable errors in the estimation of the viscoelastic pull-in parameters.

Effects of the intermolecular Casimir and vdW forces on the pull-in are compared when investigating the pull-in instability parameters of viscoelastic microbridge and microcantilever, as shown in Tables 4 and 5. Interestingly, the contribution of Casimir and vdW forces depends on the type of boundary conditions of the microactuator besides the initial gap and microactuator length. For doubly-clamped microbridge, Casimir force has greater effect on the pull-in time pull-in maximum deflection than those of vdW force. In the case of clamped-free microactuator, the pull-in time, crossponding pull-in maximum deflection are highly influenced by vdW force rather than Casimir force. These contributions of Casimir and vdW forces are also detected to steady-state time and crossponding steady-state maximum deflection. However, the difference between effects of Casimir and vdW forces on the pull-in instability parameters increases as the initial gap decreases and length of the microactuator increase

4.2.4 Effect of the durable modulus

Since the residual stress, Casimir and vdW parameters, C_R , C_C and C_{vdw} , respectively, depend on the initial Young’s modulus E_0 . Investigating the effect of the durable modulus of elasticity (E_1) on the viscoelastic pull-in response is performed considering the simultaneous effect of microstructure, electric forcing including fringing field, mid-plane stretching, residual stress and Casimir and vdW forces. The geometrical and material parameters of the viscoelastic microbridge and microcantilever are taken as those stated in Sect. 4.2 except E_1 is varied in the range from $0.2E_0$ to $0.75E_0$. Figure 13 illustrates the effect of nondimensional durable modulus $\bar{E}_1 = E_1/E_0$ on the instantaneous and durable pull-in voltages of viscoelastic microbridge and microcantilever. For both microbridge and microcantilever, it is noticed that there is no effect of \bar{E}_1 on the instantaneous pull-in voltage and so the size of the invisible (unstable) region is unchanged



◀ **Fig. 20** Effect of the nondimensional material length scale parameter l/h on the creep of the nondimensional tip deflection of viscoelastic microcantilever

by varying \bar{E}_1 . On the contrary, as \bar{E}_1 increases, the durable pull-in voltage is significantly increased and therefore a noticeable increase and decrease in the stable and durable regions, respectively, are obtained.

Creep of the nondimensional center and tip deflections of microbridge and microcantilever is shown, respectively, in Figs. 14 and 15 for various values of \bar{E}_1 . Effect of \bar{E}_1 on the nondimensional pull-in time and corresponding nondimensional maximum deflection is provided in Table 6. Again, it is noticeable that \bar{E}_1 has no effect on the instantaneous deflection for all applied voltages. In the stable region (solid lines in Figs. 14 and 15 and values with parentheses in Table 6), the time required to attain the steady-state response (t_{ss}) and corresponding steady-state deflection (w_{ss}) are distinctly increased by decreasing \bar{E}_1 . Moreover, in the durable region, decreasing \bar{E}_1 leads to a significant decrease in the pull-in time (t_{PI}), while the predicted pull-in deflection (w_{PI}) is negligibly changed. This is because of the decrease in the beam rigidity by decreasing \bar{E}_1 .

4.2.5 Effect of the relaxation time

Effect of the nondimensional relaxation time $\bar{\Psi} = 1/\Psi$ on the creep response of maximum deflections of viscoelastic microbridge and microcantilever is plotted in Figs. 16 and 17, respectively, accounting for the combined influences of microstructure, electric forcing including fringing field, mid-plane stretching, residual stress and Casimir and vdW forces. All geometrical and material parameters of the beams are the same as those stated in Sect. 4.2 except $\bar{\Psi}$ is varied in the range from 0.05 to 100. The nondimensional pull-in time and corresponding maximum deflection are displayed in Table 7 for different values of the relaxation time. It is depicted that as the relaxation time tends to zero ($\bar{\Psi}$ tends to ∞), the predicted response is exactly identical with elastic one and the microbeam reaches its final response at almost no time (i.e. at $\bar{\Psi} = 0.01 : t_{ss} = 0.121$ for microbridge at $V = 1.25V$ and $t_{ss} = 0.198$ for microcantilever at $V = 0.3V$). Also, the results show that there is no effect of the relaxation time on the instantaneous and final (steady-state or pull-in) deflection. In other words, both instantaneous and durable pull-in voltages are unaffected and consequently the microactuator

Table 8 Effect of the nondimensional material length scale parameter l/h on the nondimensional pull-in time and pull-in maximum deflection

Applied voltage (V)	Nondimensional length scale parameter l/h									
	0.0		0.25		0.50		0.75		1.0	
	$t_{PI}(t_{ss})$	$w_{PI}(w_{ss})$	$t_{PI}(t_{ss})$	$w_{PI}(w_{ss})$	$t_{PI}(t_{ss})$	$w_{PI}(w_{ss})$	$t_{PI}(t_{ss})$	$w_{PI}(w_{ss})$	$t_{PI}(t_{ss})$	$w_{PI}(w_{ss})$
Viscoelastic microbridge, $w_{PI}^c(w_{ss}^c)$										
1.2	(121.6)	(0.312)	(95.7)	(0.262)	(60)	(0.195)	(60.2)	(0.144)	(52.5)	(0.107)
1.25	15.26	0.400	(121.4)	(0.342)	(81.2)	(0.224)	(75.8)	(0.161)	(54.8)	(0.118)
1.275	6.65	0.386	29.21	0.401	(76)	(0.241)	(71.3)	(0.170)	(58)	(0.124)
1.3	1.905	0.379	13.75	0.400	(147.9)	(0.262)	(81)	(0.180)	(9115)	(90.131)
1.5	–	–	–	–	2.24	0.386	(119)	(0.319)	(89.5)	(0.194)
1.7	–	–	–	–	–	–	3.43	0.404	(146.8)	(0.337)
1.8	–	–	–	–	–	–	–	–	7.63	0.412
Viscoelastic microcantilever, $w_{PI}^t(w_{ss}^t)$										
0.3	35.48	0.524	(199)	(0.295)	(83.4)	(0.142)	(94)	(0.080)	(94.2)	(0.050)
0.35	3.41	0.489	21.6	0.513	(124.2)	(0.215)	(70.8)	(0.112)	(57.6)	(0.068)
0.4	–	–	2.09	0.464	(185.2)	(0.367)	(120.2)	(0.156)	(80.2)	(0.091)
0.5	–	–	–	–	3.69	0.482	(179.4)	(0.316)	(103.6)	(0.157)
0.6	–	–	–	–	–	–	11.67	0.501	(150.2)	(0.271)
0.7	–	–	–	–	–	–	–	–	28.31	0.536

response is unchanged from one region to another (stable, durable and unstable) by varying $\bar{\Psi}$.

The crucial role of the relaxation time is that it controls the time required to reach the final response of the microactuator; i.e. for a constant applied voltage, increasing the nondimensional relaxation time, the required time to attain the final response is increased. Interestingly, for the same applied voltage, the time required to reach the final response is almost directly proportional to the nondimensional relaxation time.

4.2.6 Effect of the length scale parameter (size effect)

To study the size effect induced by couple-stress, effect of the nondimensional material length scale parameter on the instantaneous and durable pull-in voltages, creep of the maximum deflection, pull-in time and pull-in deflection are investigated in the presence of the fringing field, mid-plane stretching, residual stress and Casimir and vdW forces. The viscoelastic material and geometrical parameters of microbridge and microcantilever are the same as those described in Sect. 4.2 except the nondimensional length scale parameter l/h is ranged from 0 to 1.

The instantaneous and durable pull-in voltages predicted by the present model (with size effect) are compared with the corresponding ones by the classical model (without size effect) as illustrated in Fig. 18. As could be seen in this figure, increasing the size scale l/h shows a significant increase in both instantaneous and durable pull-in voltages while the classical theory ($l = 0$) yields constant pull-in voltages. For large values of the size scale l/h , a significant difference between pull-in voltage predicted by the MCST and classical beam theory is obtained. For small size scales l/h , the results of MCST theory converge to those of classical theory. This behavior is attributed to that the microstructure effect (size effect) which presented by the material length scale parameter is modeled by an additional contribution on the rigidity of the microbeam.

Figures 19 and 20 show, respectively, size dependency of the creep of the nondimensional center and tip deflections of microbridge and microcantilever by considering different l/h . Table 8 gives some numerical values of the nondimensional pull-in time and crossponding nondimensional maximum deflection at various values of l/h . According to these results, at a

given applied voltage the nondimensional instantaneous deflection is distinctly decreased by increasing the size scale l/h due to the fact that increase of l/h increases the microbeam rigidity.

Also, it is worth noting that the viscoelastic pull-in response is size dependent. As the size scale l/h increases, the state of the microactuator may be changed from the unstable or durable region to the stable one. If the microbeam behaves in the stable region, increasing size scale l/h , the time required to reach the steady-state response (t_{ss}) and crossponding steady-state maximum deflection (w_{ss}) are noticeably decreased and the creep rate of the maximum deflection is increased (at $V = 1.3V$ and $V = 0.35V$ for microbridge and microcantilever, respectively when $l/h \geq 0.5$). On the other hand, at large applied voltage ($V = 1.5V$ and $V = 0.5V$ for microbridge and microcantilever, respectively), the region of the microactuator is changed from unstable region to durable or stable one by increasing the size scale l/h .

5 Conclusions

This paper investigates the size-dependent pull-in instability of nonlinear viscoelastic microcantilevers and microbridges subjected to the simultaneous effects of electrostatic actuation including fringing field, intermolecular Casimir and vdW forces, residual stress and mid-plane geometrical nonlinearity. Size effect is captured by employing the MCST in the context of linear viscoelasticity. The nonlinear integro-differential equation and boundary conditions of viscoelastic microactuators are established using the extended Hamilton principle in conjunction with Bernoulli–Euler beam theory. A modified generalized differential integral quadrature (GDIQ) method is developed for solving the governing equation together with boundary conditions. Both quasi-elastic and fully-viscoelastic solutions are obtained. The proposed model is verified against elastic and viscoelastic benchmarks and a very good agreement with previous published results is obtained. Effects of the various material and geometrical parameters on the size-dependent pull-in instability parameters of viscoelastic microbridge and microcantilever are discussed in detail in the framework of the MCST and linear viscoelastic theory. It can be concluded that:

- The viscoelastic microbridge nonlinear model considering the mid-plane stretching effect gives smaller instantaneous and durable pull-in voltages than those of linear model. Also, accounting for the mid-plane stretching effect shows a distinct increase in the pull-in time and pull-in center deflection, while a significant decrease in the steady-state (durable) center deflection and corresponding durable time is detected. Generally, the mid-plane stretching effect is increased as the initial gap increases.
- Accounting for the tensile residual stress causes an increase in the instantaneous and durable pull-in voltages of the viscoelastic microbridge. Tensile residual stress shows a decrease in the durable center deflection and durable time. On the other hand, compressive residual stress has opposite effects.
- The neglect of intermolecular Casimir and/or vdW forces may result in an overestimation of pull-in parameters of viscoelastic microbridges and microcantilevers. Such overestimation becomes much crucially with decreasing the initial gap and increasing the microactuator length. The instantaneous maximum deflection is underestimated while the pull-in time and corresponding pull-in maximum deflection are overestimated when the intermolecular forces are ignored.
- Comparing the influences of Casimir and vdW forces shows that, in the case of microbridge, Casimir force has the dominant influence on the parameters of pull-in instability, while vdW force becomes the dominant in the case of microcantilever.
- Accounting for the intermolecular forces leads to an increase in the minimum critical gap and a decrease in the detachment length of the viscoelastic microactuators.
- Without or with considering intermolecular forces, decreasing the initial gap or increasing the microactuator length shows a remarkable reduction in the instantaneous and durable pull-in voltages, pull-in time and pull-in maximum deflection while a significant increase in the steady-state time and corresponding maximum deflection is obtained.
- Increasing the durable modulus of the microactuator shows increases in the durable pull-in voltage, steady-state time and corresponding maximum

deflection, a distinct decrease in the pull-in time, a slight decrease in the pull-in maximum deflection and no effect on the instantaneous pull-in voltage and instantaneous deflection.

- Sizes of stable, durable and unstable regions of the microactuator behavior are unaffected by varying the microactuator relaxation time. The time elapsed by the microactuator to attain the steady-state or pull-in response is almost linearly proportional to the relaxation time.
- As the size scale parameter increases, the instantaneous and durable pull-in voltages are significantly increased. In the durable region, the pull-in time is obviously increased and the pull-in maximum deflection is slowly increased as the size scale parameter increases. Regardless the region of behavior, a pronounced decrease in the instantaneous deflection is detected by increasing the size effect.

Acknowledgements The author would like to thank the reviewers for their insightful comments and insight suggestions to improve the clarity of this article. The author would also like to thank Prof. Fatin F. Mahmoud and Prof. Salwa A. Mohamed (Zagazig University-Egypt) for their help in this research and for the useful discussions and advises.

References

1. Tilmans HA, Legtenberg R (1994) Electrostatically driven vacuum-encapsulated polysilicon resonators: Part II. Theory and performance. *Sens Actuators A* 45(1):67–84
2. Rezaadeh G, Tahmasebi A, Zubstov M (2006) Application of piezoelectric layers in electrostatic MEM actuators: controlling of pull-in voltage. *Microsyst Technol* 12(12):1163–1170
3. Lin W-H, Zhao Y-P (2007) Stability and bifurcation behaviour of electrostatic torsional NEMS varactor influenced by dispersion forces. *J Phys D Appl Phys* 40(6):1649
4. Das K, Batra R (2009) Symmetry breaking, snap-through and pull-in instabilities under dynamic loading of microelectromechanical shallow arches. *Smart Mater Struct* 18(11):115008
5. Batra RC, Porfiri M, Spinello D (2006) Electromechanical model of electrically actuated narrow microbeams. *J Microelectromech Syst* 15(5):1175–1189
6. Zhang W-M, Yan H, Peng Z-K, Meng G (2014) Electrostatic pull-in instability in MEMS/NEMS: a review. *Sens Actuators, A* 214:187–218
7. Mokhtari J, Farrokhbadi A, Rach R, Abadyan M (2015) Theoretical modeling of the effect of Casimir attraction on the electrostatic instability of nanowire-fabricated actuators. *Phys E* 68:149–158

8. Wineman AS, Rajagopal KR (2000) Mechanical response of polymers: an introduction. Cambridge University Press, Cambridge
9. Altenbach H, Eremeyev V (2011) Mechanics of viscoelastic plates made of FGMs. In: Computational modelling and advanced simulations. Springer, Berlin, pp 33–48
10. Fleck N, Muller G, Ashby M, Hutchinson J (1994) Strain gradient plasticity: theory and experiment. *Acta Metall Mater* 42(2):475–487
11. Fleck N, Muller G, Ashby M, Hutchinson J (1994) Strain gradient plasticity: theory and experiment. *Acta Metall Mater* 42(2):475–487
12. Kong S, Zhou S, Nie Z, Wang K (2008) The size-dependent natural frequency of Bernoulli–Euler micro-beams. *Int J Eng Sci* 46(5):427–437
13. Arash B, Wang Q (2012) A review on the application of nonlocal elastic models in modeling of carbon nanotubes and graphenes. *Comput Mater Sci* 51(1):303–313
14. Pamidighantam S, Puers R, Baert K, Tilmans HA (2002) Pull-in voltage analysis of electrostatically actuated beam structures with fixed–fixed and fixed–free end conditions. *J Micromech Microeng* 12(4):458
15. Hung ES, Senturia SD (1999) Extending the travel range of analog-tuned electrostatic actuators. *J Microelectromech Syst* 8(4):497–505
16. Xie W, Lee H, Lim S (2003) Nonlinear dynamic analysis of MEMS switches by nonlinear modal analysis. *Nonlinear Dyn* 31(3):243–256
17. Batra R, Porfiri M, Spinello D (2007) Effects of Casimir force on pull-in instability in micromembranes. *Europhys Lett* 77(2):20010
18. Ramezani A, Alasty A, Akbari J (2007) Closed-form solutions of the pull-in instability in nano-cantilevers under electrostatic and intermolecular surface forces. *Int J Solids Struct* 44(14):4925–4941
19. Zand MM, Ahmadian M (2010) Dynamic pull-in instability of electrostatically actuated beams incorporating Casimir and van der Waals forces. *Proc Inst Mech Eng Part C: J Mech Eng Sci* 224(9):2037–2047
20. Eringen AC (1972) Nonlocal polar elastic continua. *Int J Eng Sci* 10(1):1–16
21. Eringen AC (1983) On differential equations of nonlocal elasticity and solutions of screw dislocation and surface waves. *J Appl Phys* 54(9):4703–4710
22. Mindlin R, Tiersten H (1962) Effects of couple-stresses in linear elasticity. *Arch Ration Mech Anal* 11(1):415–448
23. Mindlin R, Eshel N (1968) On first strain-gradient theories in linear elasticity. *Int J Solids Struct* 4(1):109–124
24. Yang F, Chong A, Lam DCC, Tong P (2002) Couple stress based strain gradient theory for elasticity. *Int J Solids Struct* 39(10):2731–2743
25. Lam DCC, Yang F, Chong A, Wang J, Tong P (2003) Experiments and theory in strain gradient elasticity. *J Mech Phys Solids* 51(8):1477–1508
26. Rahaeifard M, Kahrobaiyan M, Asghari M, Ahmadian M (2011) Static pull-in analysis of microcantilevers based on the modified couple stress theory. *Sens Actuators, A* 171(2):370–374
27. Yin L, Qian Q, Wang L (2011) Size effect on the static behavior of electrostatically actuated microbeams. *Acta Mech Sin* 27(3):445–451
28. Kong S (2013) Size effect on pull-in behavior of electrostatically actuated microbeams based on a modified couple stress theory. *Appl Math Model* 37(12):7481–7488
29. Baghani M (2012) Analytical study on size-dependent static pull-in voltage of microcantilevers using the modified couple stress theory. *Int J Eng Sci* 54:99–105
30. Rokni H, Seethaler RJ, Milani AS, Hosseini-Hashemi S, Li X-F (2013) Analytical closed-form solutions for size-dependent static pull-in behavior in electrostatic micro-actuators via Fredholm integral equation. *Sens Actuators, A* 190:32–43
31. Zamanzadeh M, Rezaadeh G, Jafarsadeghi-Poornaki I, Shabani R (2013) Static and dynamic stability modeling of a capacitive FGM micro-beam in presence of temperature changes. *Appl Math Model* 37(10):6964–6978
32. Shaat M, Mohamed SA (2014) Nonlinear-electrostatic analysis of micro-actuated beams based on couple stress and surface elasticity theories. *Int J Mech Sci* 84:208–217
33. Shaat M, Abdelkefi A (2015) Modeling the material structure and couple stress effects of nanocrystalline silicon beams for pull-in and bio-mass sensing applications. *Int J Mech Sci* 101:280–291
34. Wang Q (2006) Axi-symmetric wave propagation of carbon nanotubes with non-local elastic shell model. *Int J Struct Stab Dyn* 6(02):285–296
35. Liang B, Zhang L, Wang B, Zhou S (2015) A variational size-dependent model for electrostatically actuated NEMS incorporating nonlinearities and Casimir force. *Phys E* 71:21–30
36. Beni YT, Karimipour I, Abadyan M (2015) Modeling the instability of electrostatic nano-bridges and nano-cantilevers using modified strain gradient theory. *Appl Math Model* 39(9):2633–2648
37. Noghrehbadi A, Eslami M (2016) Analytical study on size-dependent static pull-in analysis of clamped–clamped nano-actuators in liquid electrolytes. *Appl Math Model* 40(4):3011–3028
38. Bethe K, Baumgarten D, Frank J (1990) Creep of sensor’s elastic elements: metals versus non-metals. *Sens Actuators, A* 23(1):844–849
39. Fu Y, Zhang J, Bi R (2009) Analysis of the nonlinear dynamic stability for an electrically actuated viscoelastic microbeam. *Microsyst Technol* 15(5):763–769
40. Fu Y, Zhang J (2009) Nonlinear static and dynamic responses of an electrically actuated viscoelastic microbeam. *Acta Mech Sin* 25(2):211–218
41. Zhang J, Fu Y (2012) Pull-in analysis of electrically actuated viscoelastic microbeams based on a modified couple stress theory. *Meccanica* 47(7):1649–1658
42. Chen C, Li S, Dai L, Qian C (2014) Buckling and stability analysis of a piezoelectric viscoelastic nanobeam subjected to van der Waals forces. *Commun Nonlinear Sci Numer Simul* 19(5):1626–1637
43. Phan-Thien N (2012) Understanding viscoelasticity: an introduction to rheology. Springer, Berlin
44. Osterberg PM, Senturia SD (1997) M-TEST: a test chip for MEMS material property measurement using electrostatically actuated test structures. *J Microelectromech Syst* 6(2):107–118
45. Schapery RA (1974) Viscoelastic behavior and analysis of composite materials. *Mechanics of composite materials (A*

- 75-24868 10-39). Academic Press Inc., New York, pp 85–168
46. Chen L, Zhang W, Liu Y (2007) Modeling of nonlinear oscillations for viscoelastic moving belt using generalized Hamilton's principle. *J Vib Acoust* 129(1):128–132
 47. Nayfeh AH, Emam SA (2008) Exact solution and stability of postbuckling configurations of beams. *Nonlinear Dyn* 54(4):395–408
 48. Huang J-M, Liu A, Lu C, Ahn J (2003) Mechanical characterization of micromachined capacitive switches: design consideration and experimental verification. *Sens Actuators, A* 108(1):36–48
 49. Gusso A, Delben GJ (2008) Dispersion force for materials relevant for micro-and nanodevices fabrication. *J Phys D Appl Phys* 41(17):175405
 50. Batra R, Porfiri M, Spinello D (2008) Vibrations of narrow microbeams predeformed by an electric field. *J Sound Vib* 309(3):600–612
 51. Attia MA, Mahmoud FF (2016) Analysis of viscoelastic Bernoulli-Euler nanobeams incorporating nonlocal and microstructure effects. *Int J Mech Mater Des* 1–12. doi:[10.1007/s10999-016-9343-4](https://doi.org/10.1007/s10999-016-9343-4)
 52. Shu C (2012) *Differential quadrature and its application in engineering*. Springer, Berlin
 53. Attia MA, Mohamed SA (2016) Nonlinear modeling and analysis of electrically actuated viscoelastic microbeams based on the modified couple stress theory. *Appl Math Model*. doi:[10.1016/j.apm.2016.08.036](https://doi.org/10.1016/j.apm.2016.08.036)
 54. Schapery RA (1965) A method of viscoelastic stress analysis using elastic solutions. *J Franklin Inst* 279(4):268–289
 55. Nayfeh AH, Mook DT (2008) *Nonlinear oscillations*. Wiley, London
 56. Kahn H, Heuer AH (2002) Thermal stability of residual stresses and residual stress gradients in multilayer LPCVD polysilicon films. *J Ceram Process Res* 3(1):22–24